ORIGINAL PAPER

Investigation of experimental results and *D*-optimal design of hafnium ion extraction from aqueous system using emulsion liquid membrane technique

Iman Salahshoori[1] · Ali Hatami[1] · Ahmad Seyfaee[2]

Abstract

Hafnium metal is used in a wide range of industries such as microprocessor manufacturing, nuclear reactors and special alloys due to its physical, chemical and radiation properties. Emulsion liquid membrane (ELM) is an effective and efficient alternative for heavy metal separation compared to conventional methods due to high selectivity, energy-saving, high mass transfer and low operating capital. In this study, Cyanex 572 as a carrier, Span 85 as a surfactant, hydrochloric acid as an internal phase and kerosene as a diluent were used. In the first part of the study, the stability of the emulsions was investigated. The most stable emulsions were obtained by adding PIB polymer (3% w/v), Span 85 surfactant (3% w/v) and stirring for 15 min. In the second part, the separation of hafnium metal ions from aqueous solutions was investigated using ELM technique. The highest separation was obtained at 4% (v/v) as carrier concentration, 4% (w/v) as surfactant concentration, the membrane-to-feed volume ratio of 20/100 and W/O/W emulsion stirring rate and time equal to 400 rpm and 5 min, respectively. Moreover, to optimize the factors influencing the tests, the design of experiment (DOE) was performed using *D*-optimal method via Design Expert 10 software. Based on DOE results, the maximum extraction (> 99%) was achieved when the carrier concentration, the surfactant concentration, W/O/W emulsion stirring time, W/O/W emulsion stirring rate and emulsion volume/feed phase ratio were 4.49% v/v, 3.90% w/v, 11.49 min, 310.54 rpm and 2:1, respectively.

Keywords Hafnium ion · *D*-optimal design · Emulsion liquid membrane · Design of experiment

Introduction

With the development of different industries, an increase in the separation process efficiency and a decrease in the energy consumption of the separation process have become important goals of any separation technique. Therefore, it is important to select a suitable separation method or develop and study innovative techniques which are accessible and easy to construct and have the potential to meet the above-mentioned goals [1].

Membrane separation has gained much attention due to its cost-effectiveness. However, to date, membrane processes have found little industrial applications. The reasons for this can be due to its low separation rate and selectivity [2–5]. Nonetheless, to further improve the separation efficiency, a newer method has been developed. In this method, very high separation efficiency is achieved by employing liquid membranes with the aid of special agents (carriers) which facilitate the mass transfer of the specific component for separation [6].

The emulsion liquid membrane (ELM) has advantages over other methods that make it preferable. These advantages include less energy requirement, high separation selectivity, high mass transfer rate and less residence time [7]. To date, ELM technique has been used for the separation of many materials such as phenol [8], amino acids [9] and metals such as silver [10], gold [11], molybdenum [12], arsenic [13], platinum [14], rhodium [15], cadmium [16], cobalt [17], copper [18, 19], uranium [20], palladium [21], chromium [22], zinc [23], zirconium [24] neodymium and gadolinium [25].

✉ Iman Salahshoori
  iman.salahshoori@srbiau.ac.ir; iman.salahshoori@gmail.com

1 Department of Chemical Engineering, Science and Research Branch, Islamic Azad University, Tehran, Iran

2 School of Mechanical Engineering, University of Adelaide, Adelaide, Australia

The ELM system consists of the internal phase as the striping phase, the external phase as the feed phase and the membrane phase (carrier, diluent and surfactant). The general method in this technique is to first mix the internal phase and the membrane phase using a high-speed homogenizer, and then after forming a stable emulsion, it would be placed in the external phase for separation. Finally, the de-emulsification operation is performed on the emulsion, and the membrane phase enters the emulsification process for reuse [26]. Figure 1 shows an overview of this process.

Hafnium metal has important applications in gas and electric lights manufacturing, radiation control in nuclear reactors, refining oxygen and nitrogen, and in the durability improvement of refractory metals such as tungsten and tantalum. In regard to the environmental impacts of Hf, it is stated that its dust increases the risk of fire and explosion [27–29]. Until now, hafnium extraction has been performed in several ways such as liquid–liquid extraction [30], hydrogen plasma arc melting [31], resins [32, 33] and hollow fiber renewal liquid membrane technique [24]. So far, various carriers such as Ionquest 801 [34], benzyl alcohol [35], di-n-butyl sulfoxide (DBSO) [36], Cyanex 921, Cyanex 923, Cyanex 925 [37], DEHPA, Cyanex 272, TBP, Primene JTM, Alamine 336 and Aliquat 336 [38], TOP, DOS, D2EHPA

[39], PC 88A, Lix 63 [40] have been used to extract hafnium ions. However, to the best of our knowledge, the extraction of the Hf metal via the emulsion liquid membrane using the Cyanex 572 carrier has not been reported so far. Cyanex 572 carrier is a highly stable phosphorus-based chelating carrier which has been specially formulated for the extraction and purification of rare earth elements. Table 1 shows the physical properties of Cyanex 572. It is stated that Cyanex 572 carrier has more advantages over the traditional phosphonic acid carriers [41, 42].

In this study, first, the important factors affecting the extraction process of hafnium ions were investigated using ELM technique. Then, response surface methodology (RSM) was used to find levels of factors influencing the test

Table 1 Physical properties of Cyanex 572

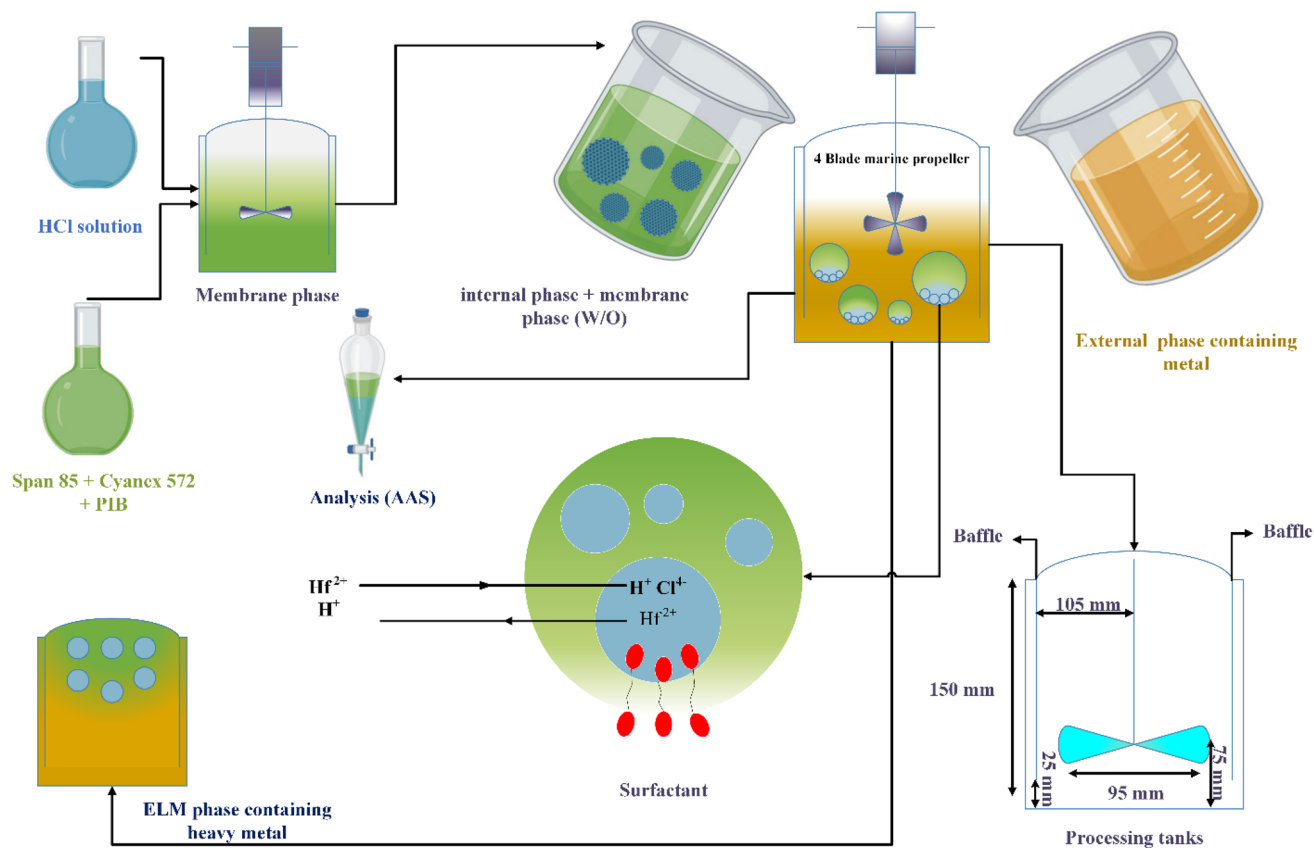| Sample	Physical properties of Cyanex 572
Appearance (clarity)	Colorless to light amber liquid
Specific gravity	0.93–0.95 g/cm^3
Viscosity 25 ^{o}C	< 50 CP
Viscosity 50 ^{o}C	< 25 CP
Active strength	> 2.9 M

Fig. 1 A schematic diagram of the emulsion liquid membrane process

process. Finally, among the experimental design methods in RSM, the *D*-optimal design method was used to find the optimized operational condition.

Material and method

Chemicals

Hafnium(IV) chloride (Merck) and hydrochloric acid (Merck) were used as external and internal phases, respectively. The sorbitan trioleate emulsifier ($C_{60} H_{108} O_8$, MW = 957.51 g/mol from Sigma-Aldrich) or equivalently Span 85 was used as the emulsion stabilizer. The polyisobutylene (PIB, Sigma-Aldrich) with a molecular weight of 125,0000 was used as the additive polymer (non-Newtonian fluid). Cyanex 572 (Cytec Canada) was used as the carrier. Kerosene from Sigma-Aldrich was used as the diluent in the organic phase, and sulfuric acid, sodium hydroxide and nitric acid (Merck) were used for pH adjustment. In addition, deionized water was used during the testing process.

Apparatus

The laboratory homogenizer T25 digital Ultra-Turrax Model IKA with a range of 2500–24,000 rpm was used to make the initial emulsion. A SHIN SAENG Model SDS-41D laboratory mixer made in Korea was used to stir the solutions during extraction. Inductively coupled plasma atomic emission spectroscopy (optima 7300 DV, Perkin Elmer) was used to determine the concentration of hafnium ions in feed samples. The pH meter 3505 Jenway was used to measure the pH of aqueous solutions. KOKUSAN H-11n centrifuge was used to break the ELM and separate the organic phase from the external phase. Cylindrical glass container 90 mm in diameter and 150 mm high was used, which is equipped with four 4-mm diameter glass bars as a baffle to cause turbulences. A 4-blade propeller with a blade angle of 45 degrees relative to its central axis, and a diameter equal to 25 mm and a width of 9 mm was used to stir the solutions during extraction.

The digital scale of RADWAG model AS 220/C/2 was used for weighing chemicals in all experiments. A shaking water bath model SWBR27 made by SHEL LAB was used to mix the chemicals in an isothermal environment. The Malvern Zen 3600 Zetasizer dynamic light scattering instrument was used to measure the size of the emulsions in the liquid phase.

Experimental procedure

Initially, the external phase was prepared by dissolving 0.178 g hafnium chloride in 100 ml water (100 ppm molar). External phase pH was adjusted using nitric acid or sodium hydroxide.

The membrane phase was prepared by mixing a certain amount of organic phase including Cyanex 572 (concentration in the organic phase 0–6 v/v %) as the carrier and Span 85 as the emulsifier (concentration in the organic phase 1–5 w/v %) with kerosene as the diluent (total volume ~ 100 ml). The mixture was introduced to the homogenizer. During mixing, to improve the membrane stability, 5 ml of a prepared mixture of PIB in kerosene (concentration ranging 1–4% w/v) was added slowly to the homogenizer (at 10,000 rpm) and stirred for 5 to 25 min. To form the emulsion, the internal phase (hydrochloric acid (HCl) in deionized water with concentration ranging from 0.2 to 1 M) was added dropwise to the homogenizer containing the organic phase. Finally, 100 ml of the formed W/O emulsion was added to 500 ml of the external phase solution (feed phase) under mild stirring condition (ranging from 250 to 450 rpm) and formed the emulsion liquid membrane (ELM).

Analytical method

At different times, a sample of the W/O/W was taken (~ 10 ml) and transported to a separator funnel where enough time was given to the emulsion to separate into organic-rich and aqueous-rich phases. The phases were carefully separated and transferred to two different measuring cylinders, and their volumes were measured. The organic-rich phase was heated to break the W/O emulsion and form two phases: organic and aqueous. The volume of each phase was measured after the separation. The emulsion swelling, the extraction fraction and the enrichment are calculated using Eqs. 1–3 [43]:

$$\text{Emulsion swollen percentage}: \text{Sw}(\%) = \left(\frac{V_\text{f} - V_\text{i}^0}{V_\text{i}^0} \right) \times 100 \tag{1}$$

$$\text{Extraction fraction}: E = \frac{C_0^e - C_\text{f}^e}{C_0^e} \tag{2}$$

$$\text{Enrichment}: C_\text{En} = \frac{C_\text{f}^\text{i}}{C_0^e} \tag{3}$$

where V_i^0 and V_f are the initial volume and the final volume of the internal phase, respectively. C_0^e and C_f^i are the initial and the final concentration of the metal ion in the external and internal phases in ppm, respectively.

The emulsion stability is calculated using the membrane leakage percentage via the following formula:

$$\text{Leakage} = \frac{V_\text{R}}{V_\text{i}^0} \times 100 \tag{4}$$

where V_R is the volume of the leaked internal phase to the external phase and calculated via the following relation:

$$V_\text{R} = V_e^0 \times \frac{10^{\text{pH}_e^0} - 10^{\text{pH}_e^t}}{10^{\text{pH}_e^t} - \text{C}_{\text{H+,i}}^0} \tag{5}$$

V_e^0 is the initial volume of the external phase, $\text{C}_{\text{H+,i}}^0$ is the initial concentration of H$^+$ in the internal phase, pH_e^0 is the initial pH of the external phase, and pH_e^t is the external phase pH collected via the separating funnel at any sampling time (t).

Results and discussion

Membrane stability

Preparing a preliminary emulsion (W/O) that does not break in contact with the external phase is a major factor in the successful fabrication of any emulsion liquid membrane. Unfortunately, the widespread use of the emulsion liquid membrane is limited due to the instability of the emulsion globules. With the breakdown of emulsion globules, the internal phase mixes with the external phase, which reduces the extraction efficiency. Therefore, membrane stability improvement is one of the most important aspects of ELM [44–46]. Several methods have been reported to improve the stability of the emulsion liquid membrane; the most important factors are: (1) to increase emulsifier concentration, (2) to increase membrane viscosity and (3) using a non-Newtonian diluent as the membrane medium. Moreover, factors such as emulsification time, type and amount of surfactant, type and concentration of the internal phase, and the volume ratio of the internal phase to the membrane phase impact the membrane stability [47, 48]. Park et al. [49] examined a stable emulsion by substituting the membrane medium with a non-Newtonian fluid to separate benzoic acid from the external phase. The results showed that with an increase in polyisobutylene polymer concentration from 0.5 to 1.5%, and an increase in viscosity from 4.2 to 43 cP, the extraction fraction reached more than 0.96. In another study, Barad et al. [50] investigated the stability of ELM in the extraction of aromatic amines by changing various parameters such as emulsifier concentration, acidic internal phase concentration and mixing rate. They reported that by increasing the concentration of acid in the internal phase from 0.1 to 1 N, emulsion swelling increased. In addition, by examining the various concentrations of emulsifiers, they found that at

low concentrations of emulsifiers (less than 3% w/v) the emulsions were stable for a short time, which increased when concentration of emulsifiers increased to 7%.

In this study, a solution of HCl was used as the internal phase (striping phase). Membrane stability is evaluated by the membrane leakage method and the effect of each variable (e.g., polymer and surfactant concentration, emulsification time, internal phase concentration and internal-to-oil volume ratio) on the emulsion stability is investigated.

The effect of polymer concentration

There are two opposite phenomena related to an increase in polymer concentration. On the one hand, the membrane stability is improved (due to increased membrane viscosity) by polymer concentration. On the other hand, an increase in the polymer concentration increases the mass transfer resistance [44, 51]. The addition of polymer causes the membrane phase to change its rheology from Newtonian fluid to non-Newtonian fluid. Skelland suggested, for the first time, that the conversion of the membrane phase from Newtonian to non-Newtonian liquid by the addition could occur upon the addition of polymer. Adding a suitable polymer to the membrane phase is a new technique that would increase the stability of ELM without a significant reduction in permeability of the membrane [52]. One of the predominant benefits of polymer in the formulation of emulsions is its recyclability. The recovery of the polymer can be achieved without any changes in its property. Brugger and Richtering stated that poly(N-isopropylacrylamide)-comethacrylic acid polymers improve the stability of the emulsions significantly [53].

Lee and Yeo studied the role of a dilute polymer solution on the stability of the emulsion. They stated that addition of a small quantity of polymer reduced the emulsion swelling without affecting the extraction [54]. Mortaheb et al. used a new polyamine-type surfactant for the extraction of phenol by ELM from aqueous solutions and showed that the new surfactant was more efficient than Span 80 that is widely used in ELM systems [55, 56]. Figure 2 shows that increasing the polymer concentration (PIB) from 1 to 3% (w/v) increases emulsion stability. However, by increasing the polymer concentration to values greater than 3% (w/v), the leakage increased. The reason could be due to interactions between PIB and Span 80. The decrease in the membrane stability with further increase in PIB concentration could be due to the migration of surfactants from the interface of the aqueous phase and organic phase due to an increase in the steric effects of PIB. In addition, experiments without the polymer showed that in general, the leakage increased with time compared to experiments in which PIB was used [57].
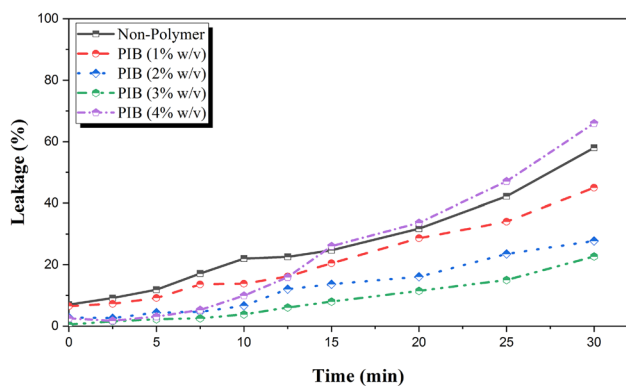
Fig. 2 Effect of polymer (PIB) concentration on the stability of ELM (Cyanex 572: 4.5% (v/v), internal phase HCl concentration: 0.8 M, mixing rate: 400 rpm, Hf concentration in the external (feed) phase: 100 ppm, emulsification time: 15 min, internal phase-to-membrane phase volume ratio: 1/1, emulsion-to-external phase volume ratio: 20/100, surfactant concentration: 3% (w/v))

Effect of surfactant concentration

In the ELM process, on the one hand, the surfactants stabilize the membrane. On the other hand, the concentration of surfactant adversely affects the extraction efficiency by reducing the solutes' mass transfer from the external phase into the internal phase within emulsion globules [58]. The layer formed by the surfactant between the aqueous phase and the organic phase controls the emulsion stability. As the surfactant concentration increases, more molecules migrate to the interface of the aqueous phase and the organic phase. Generally, the higher the surfactant concentration, the greater the mass transfer resistance at the interface and lower membrane permeability and leakage [59].
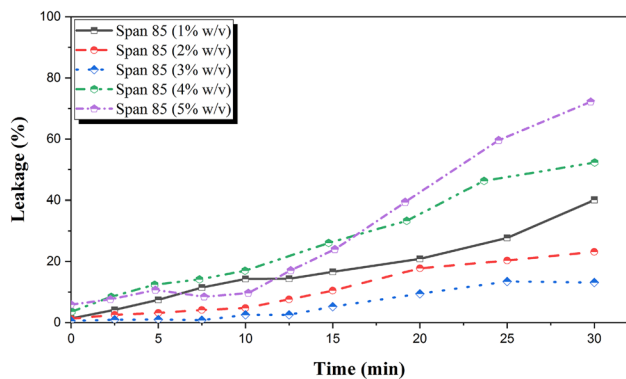
The effect of Span 85 surfactant concentration on W/O emulsion stability is shown in Fig. 3. As can be seen in the figure at low surfactant concentrations, the emulsion is less stable, which may be contributed to the lack of stabilizing agents at the interface of external phase and globules. However, this trend was not monotonic, and by increasing the surfactant concentration to values greater than 3% (w/v), the emulsion stability decreased. The decrease in the stability may be attributed to an increase in the steric effects between surfactant pair molecules and surfactants and PIB pair molecules, which could lead to the migration of some of the surfactant molecules from the interface of the organic phase and feed phase and forming reversed micelles in the aqueous phase. The formed reversed micelles could destabilize the
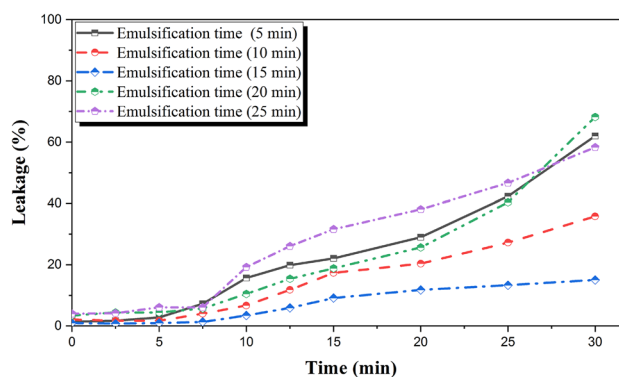

Fig. 4 Effect of emulsification time on the stability of ELM (Cyanex 572: 4.5% (v/v), internal phase HCl concentration: 0.8 M, mixing rate: 400 rpm, Hf concentration in the external (feed) phase: 100 ppm, internal phase-to-membrane phase volume ratio: 1/1, emulsion-to-external phase volume ratio: 20/100, PIB: 3% (w/v), surfactant concentration: 3% (w/v))

Fig. 3 Effect of surfactant (Span 85) concentration on the stability of ELM (Cyanex 572: 4.5% (v/v), internal phase HCl concentration: 0.8 M, mixing rate: 400 rpm, Hf concentration in the external (feed) phase: 100 ppm, emulsification time: 15 min, internal phase-to-membrane phase volume ratio: 1/1, emulsion-to-external phase volume ratio: 20/100, PIB: 3% (w/v))

Fig. 5 Effect of HCl concentration in the internal phase on the stability of ELM (Cyanex 572: 4.5% (v/v), mixing rate: 400 rpm, Hf concentration in the external (feed) phase: 100 ppm, emulsification time: 15 min, internal phase-to-membrane phase volume ratio: 1/1, emulsion-to-external phase volume ratio: 20/100, PIB 3% (w/v), surfactant concentration: 3% (w/v))
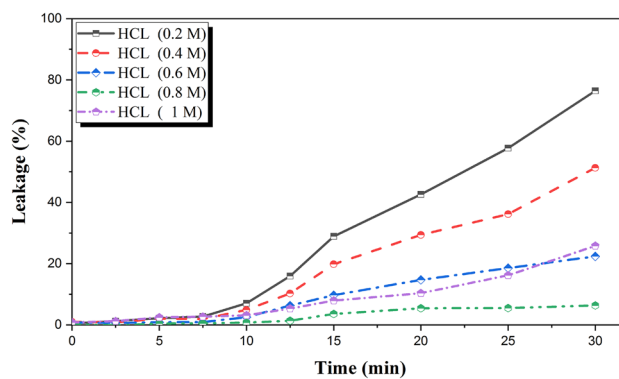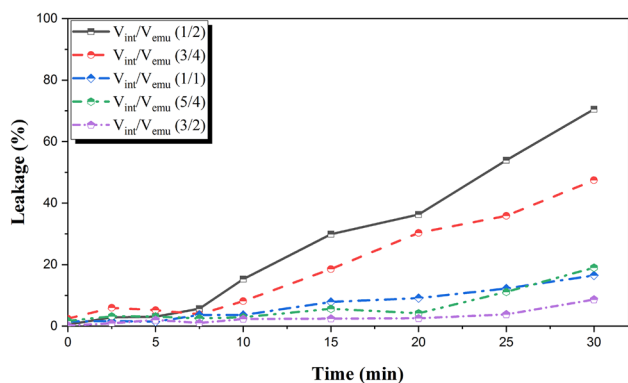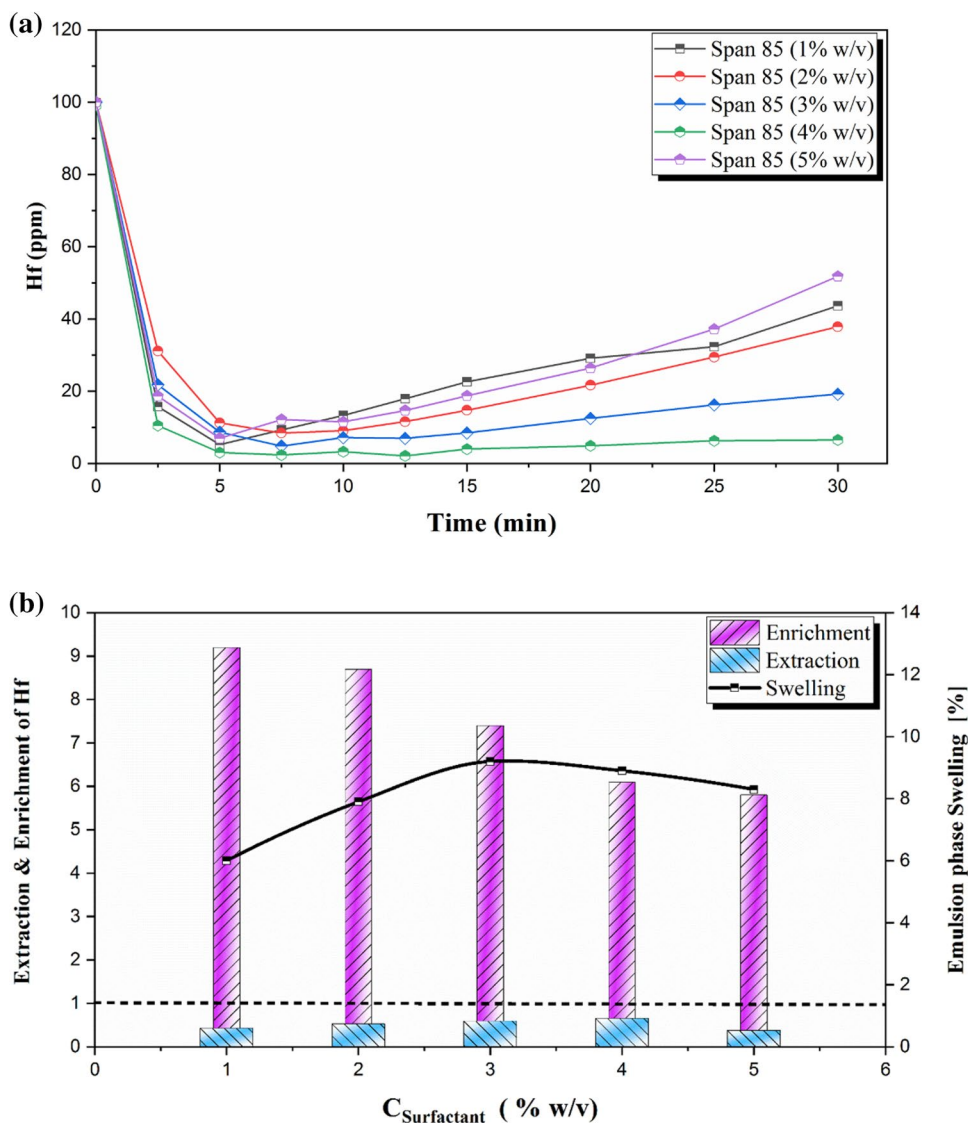
Fig. 6 Effect of phase ratio on stability of ELM (Cyanex 572: 4.5% (v/v), mixing rate: 400 rpm, Hf concentration in the external (feed) phase: 100 ppm, emulsification time: 15 min, internal phase HCl concentration: 0.8 M, emulsion-to-external phase volume ratio: 20/100, PIB: 3% (w/v), surfactant concentration: 3% (w/v))

membrane phase via interaction with oil droplets. Moreover, an increase in the surfactant concentration could lead to an increase in the osmotic pressure of the internal phase, followed by swelling and potentially the breakage of the membrane phase (e.g., increase in the leakage) [60, 61].

It is noteworthy that at high surfactant concentrations, the surfactant acts as a barrier at the interface interfering the formation of carrier–solute complex and therefore, decreasing the extraction rate [62]. The results showed that the optimum concentration of surfactant was 3% w/v.

Effect of emulsification time

Experiments with emulsification time from 0 to 30 min were conducted to determine the effect of emulsion mixing time on membrane stability. The results are demonstrated in Fig. 4 and show that for emulsion mixing time less than 10 min, the emulsion was less stable and broke down quicker

Fig. 7 Effect of surfactant (Span 85) concentration on the **a** final Hf concentration in the external phase and **b** extraction and enrichment of Hf and swelling ratio of ELM (Cyanex 572: 4.5% (v/v), internal phase HCl concentration: 0.8 M, mixing rate: 400 rpm, Hf concentration in the external (feed) phase: 100 ppm, emulsification time: 15 min, internal phase-to-membrane phase volume ratio: 1/1, emulsion-to-external phase volume ratio: 20/100, PIB: 3% (w/v))

compared to more extended emulsion mixing time tests. The observed instability could be due to the less homogenization extent of the internal phase with the membrane phase. Also for 10-min emulsion mixing time data point, the emulsion droplet size was large, which facilitated the membrane leakage. In contrast, increasing the emulsification time to values greater than 10 and smaller than 15 min, the highest emulsion stability was obtained. This could be due to a better homogenization of internal and membrane phases compared to cases with lower emulsification time. However, it was observed that by increasing the mixing time beyond 15 min, the emulsion stability decreased. The observed decrease in the emulsion stability may be attributed to the formation of new interfaces (due to an increase in the number density of droplets), hence causing a shortage in the available surfactant molecules per unit area of the droplets [60, 63–65]. As a result, the emulsion mixing time equal to 15 min was chosen.

Effect of internal phase concentration

Another effective parameter on the emulsion stability is the concentration of the internal phase (stripping) [66]. Figure 5 shows the effect of internal phase concentration on emulsion stability. The results in Fig. 5 show that on the one hand, increasing the internal phase concentration from 0.2 to 0.8 M increases the emulsion stability. On the other hand, the membrane stability decreases with further increase in the concentration of HCl solution from 0.8 to 1 M. It should be noted that at high concentrations of HCl, the decrease in emulsion stability may be due to the increased interaction between HCL and surfactant. Therefore, an increase in the concentration of the internal phase causes the osmotic swelling of the internal phase (stripping) resulting in destabilization of the emulsion [67]. The optimum concentration of the internal phase to yield a stable emulsion was found to be equal to 0.8 M.

Fig. 8 Effect of carrier (Cyanex 572) concentration on the **a** final Hf concentration in the external phase and **b** extraction and enrichment of Hf and swelling ratio of ELM (internal phase HCl concentration: 0.8 M, mixing rate: 400 rpm, Hf concentration in the external (feed) phase: 100 ppm, emulsification time: 15 min, internal phase-to-membrane phase volume ratio: 1/1, emulsion-to-external phase volume ratio: 20/100, surfactant concentration: 3% (w/v), PIB: 3% (w/v))
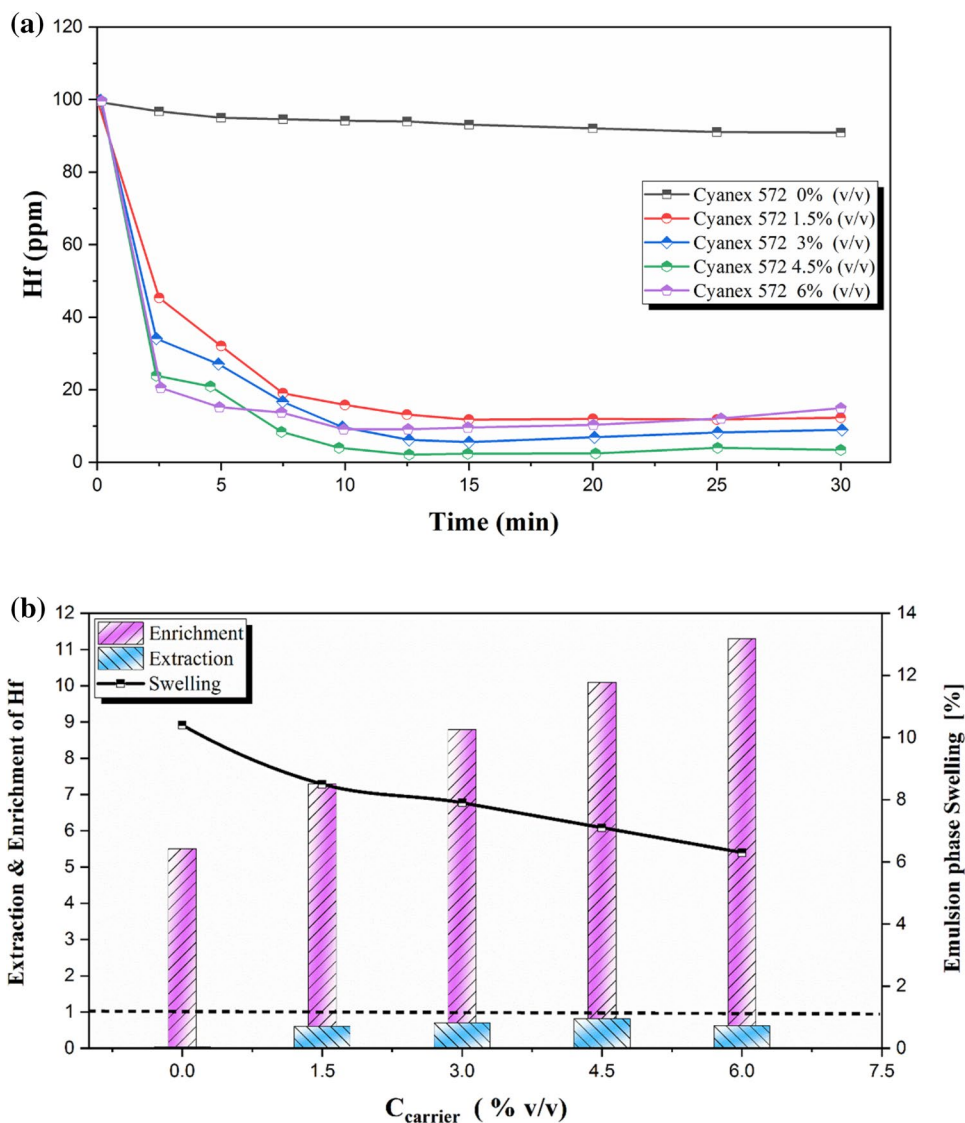
Effect of internal phase-to-membrane phase volume ratio

The effect of the ratio of internal phase volume to membrane phase volume on W/O stability is shown in Fig. 6. As shown in Fig. 6, the stability of the emulsion increases with an increasing volume ratio of phases. Although it may seem reasonable to choose 1:1 volume ratio as the optimum condition for W/O/W cases, one should note that an increase in the volume ratio of the internal phase has an inverse effect on the stability and extraction of in ELM process. It is stated that an increase in the volume ratio of the internal phase to the emulsion phase causes an increase in the average size of the droplets as well as a stretch in the size distribution extent of globules. This would decrease the interfacial contact area between the emulsion and the external phase and hence, decreases the extraction efficiency. Moreover, in high volume ratio experiments, the amount of the organic phase

may not be enough to embed all the internal aqueous phase, which in turn make the dispersion of W/O emulsion in the external phase to be more challenging. Therefore, to prepare a less challenging dispersion in the synthesis of W/O/W emulsion, which contains more uniform globule size, the ratio of 1:1 was considered [60, 68, 69].

Extraction of Hafnium ions by emulsion liquid membrane method

Effect of surfactant concentration

As stated in the previous section (emulsion stability), the primary role of surfactants in the emulsion structure is to enhance emulsion stability. The emulsion stability is a strong function of the type and concentration of surfactants and affects the performance of metal ion extraction

Fig. 9 Effect of emulsion-to-external phase volume ratio on the **a** final Hf concentration in the external phase and **b** extraction and enrichment of Hf and swelling ratio of ELM (Cyanex 572: 4.5% (v/v), internal phase HCl concentration: 0.8 M, mixing rate: 400 rpm, Hf concentration in the external (feed) phase: 100 ppm, emulsification time: 15 min, internal phase-to-membrane phase volume ratio: 1/1, surfactant concentration: 3% (w/v), PIB: 3% (w/v))
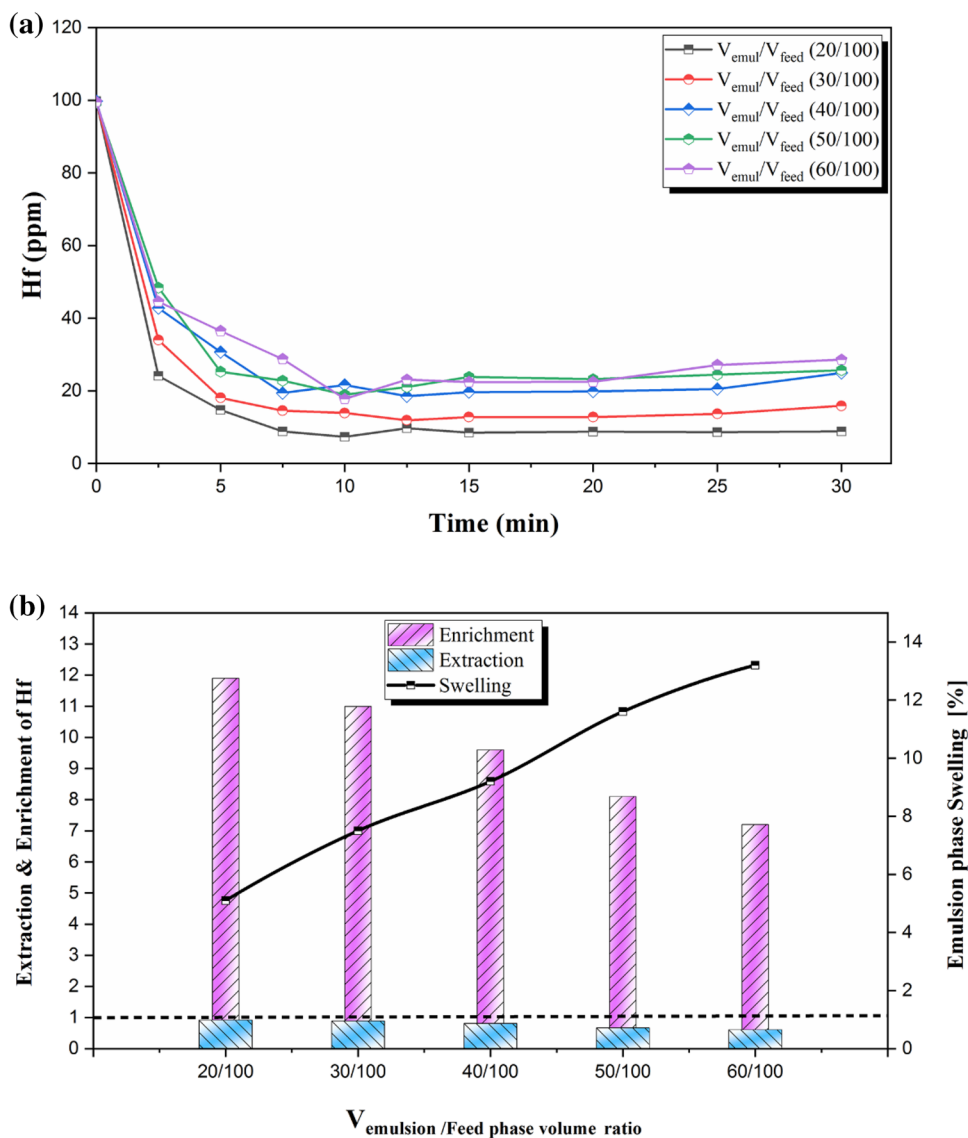
in the emulsion liquid membrane (ELM) method [47]. In this research, Span 85 and the polyisobutylene (PIB) were employed to improve the emulsion stability. Surfactant concentrations have a two-way effect on the rate of metal ion extraction.

On the one hand, increasing the concentration of surfactant increases the emulsion stability by decreasing the surface tension between the phases. On the other hand, an increase in the surfactant concentration increases the viscosity of the membrane [58]. Therefore, although the membrane stability enhances, its viscosity would increase at the same time. An increase in the viscosity leads to a reduction in both the diffusion coefficient and the relative carrier concentration (at the interface) which subsequently leads to a reduction in the mass transfer rate of the metal ions in the membrane phase.

According to Fig. 7a, by increasing the surfactant concentration (Span 85) from 1 to 4%, the extraction rate is increased. However, by increasing the Span 85 concentration beyond 4%, the separation rate decreases due to the addition of an extra mass transfer resistance on the interface of the membrane and the external phases that interferes with the formation of the carrier–solute complex [70].

In addition, it can be stated from Fig. 7b that as the concentration of surfactant passes ~ 3 w/v%, the carrier–solute complex should overcome more resistance (due to an increase in the steric effect of surfactant on the internal phase interface) to release its content in the internal phase. Therefore, the separation efficiency decreases with further increase in the concentration of the surface-active reagents. Moreover, the results showed that the penetration of water from the external phase to the internal phase and hence, swelling increased with an increase in the surfactant concentration, and therefore decreased the enrichment [71].

Fig. 10 Effect of W/O/W emulsion mixing rate on the **a** final Hf concentration in the external phase and **b** extraction and enrichment of Hf and swelling ratio of ELM (Cyanex 572: 4.5% (v/v), internal phase HCl concentration: 0.8 M, Hf concentration in the external (feed) phase: 100 ppm, emulsification time: 15 min, internal phase-to-membrane phase volume ratio: 1/1, emulsion-to-external phase volume ratio: 20/100, surfactant concentration: 3% (w/v), PIB: 3% (w/v))
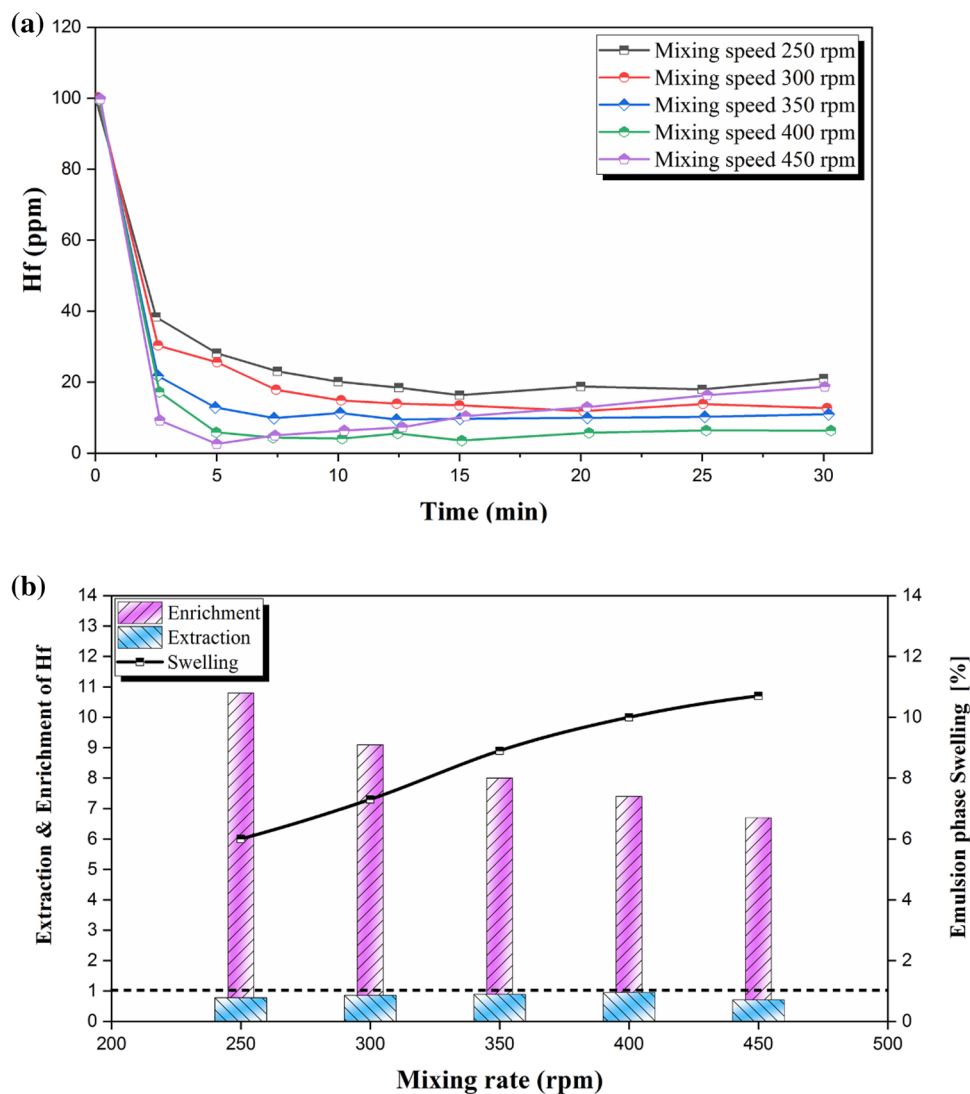
Effect of carrier concentration

A carrier and its complex with the desired component should be soluble in the membrane phase but insoluble in the internal and external phases [72]. In general, the presence of carrier material in the liquid membrane controls the extraction efficiency of the target component as carriers transport Hf ions through the membrane. In this study, Cyanex 572 as a chelating carrier suitable for the separation of rare metals was used. It is claimed that Cyanex 572 carrier is more advantages over the traditional phosphonic acid carrier [73]. The effect of Cyanex 572 extractant concentration on Hf ion extraction using ELM technique is shown in Fig. 8a. As the concentration of carrier material increased from 0 to 4.5 vol%, the extraction fraction increased.

However, when the carrier concentration was ∼ 6 vol%, the extraction rate decreased. The amount of carrier material directly affected the complex formation rate, thereby increasing the mass transfer rate. Nevertheless, at high concentrations, the carrier molecules adsorb competitively with the surfactant molecules at the interface of the internal phase and the membrane phase, increasing the interfacial tension and the internal droplet diameter, reducing the mass transfer coefficient and ultimately the mass transfer rate. Figure 8b shows the effect of carrier concentration on extraction, enrichment and emulsion swelling. As expected, the enrichment increased as the carrier concentration increased. Because of the higher carrier content inside the membrane, more complexation with the dissolved material was created and, therefore, the enrichment increases. Since the carrier material is insoluble in water, it can act as a barrier to water entry and reduce the system swelling. Therefore, at high concentrations of the carrier material, the system swelling decreases [2].

The effect of the emulsion/feed phase volume ratio

The membrane-to-feed phase volume ratio has two counter effects. On the one hand, increasing this ratio increases the membrane thickness, which leads to an increase in emulsion

Fig. 11 Effect of W/O/W emulsion stirring time on the **a** extraction, enrichment of Hf and swelling ratio of ELM (Cyanex 572: 4.5% (v/v), internal phase HCl concentration: 0.8 M, Hf concentration in the external (feed) phase: 100 ppm, emulsification time: 15 min, mixing rate: 400 rpm, internal phase-to-membrane phase volume ratio: 1/1, emulsion-to-external phase volume ratio: 20/100, surfactant concentration: 3% (w/v), PIB: 3% (w/v)) and **b** emulsion size distribution measured by DLS
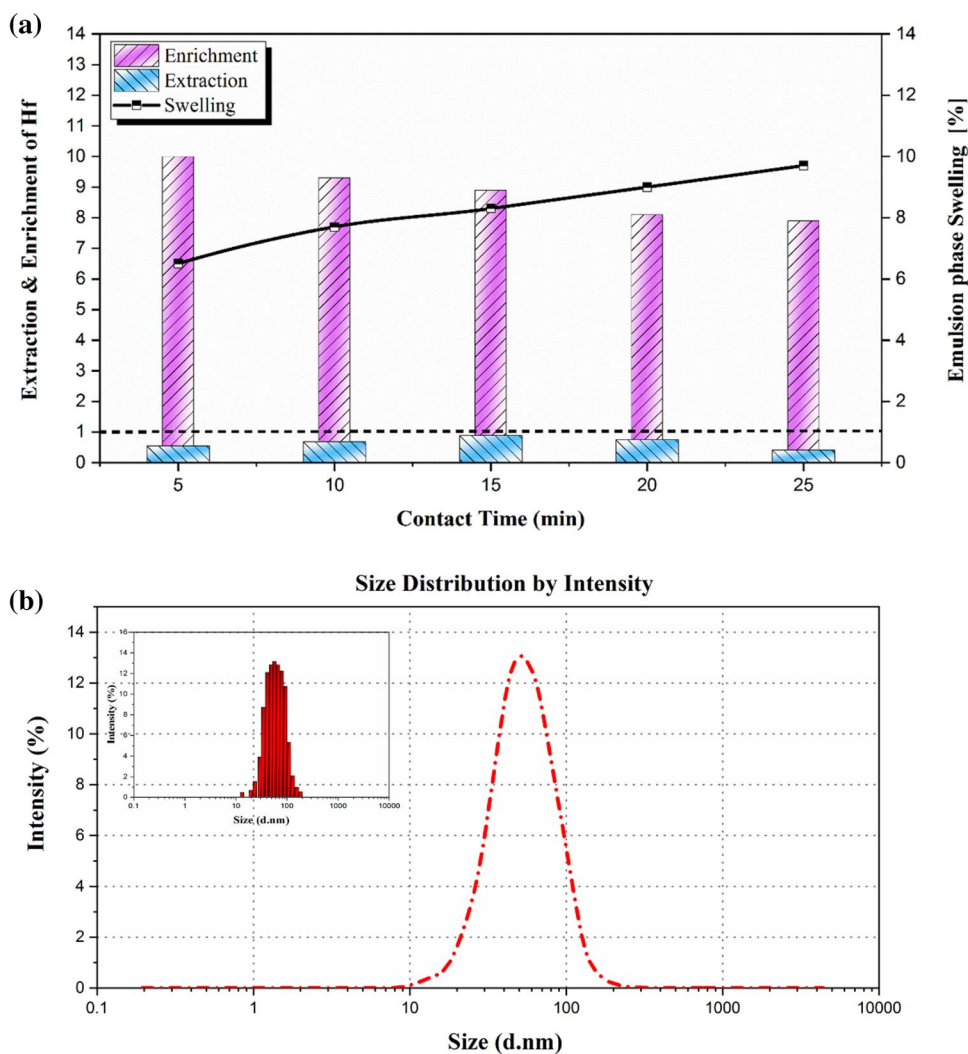
stability. On the other hand, it reduces the mass transfer coefficient and reduces the extraction rate [47]. The effect of the emulsion to the feed (external) phase volume ratio is presented in Fig. 9a. The results show that as the emulsion-to-external phase volume ratio increases, the emulsion swells and the extraction rate decreases. The effect of the emulsion-to-external phase volume ratio on enrichment and emulsion swelling is shown in Fig. 9b. As can be seen from Fig. 9b, higher volume ratios resulted in a higher internal phase swelling, a higher internal phase dilution and a decrease in the enrichment [61].

Effect of W/O/W emulsion stirring speed

One of the most important factors affecting the membrane stability and extraction efficiency in the ELM process is the mixing rate and the intensity of the turbulence in the external phase, which directly affects the mass transfer of solute in the system [74]. Proper stirring should be able to disperse the emulsions into separated droplets throughout the external phase and create a uniform distribution of the emulsified cells. This would potentially maximize the contact between the emulsion phase and the external phase, which would increase the extraction efficiency. In order to achieve this, in addition to using the proper stirring rate, the location of the stirrer blade inside the external phase is also important [75]. Investigations in this work showed that the best place to place the stirrer blade is within the lower third of the solution, in which case it can disperse the cells throughout the external phase. Increasing the stirring rate in the extraction step can have two opposite effects [76]. On the one hand, an increase in stirring rate can increase the dispersity of the emulsion cells and reduce the average emulsion droplet size in the external phase. On the other hand, this increase in the stirring rate can increase the breakage/coalescence rate of the emulsion cells due to an increase in the collision rate between the cells. As can be seen in Fig. 10a, with increasing mechanical stirrer rate from 250 to 400 rpm, the extraction rate increases and as the stirrer speed increases, the extraction enters a downward trend. In fact, as the stirrer speed increases, the diameter of the formed globules initially decreases, followed by the mass transfer coefficient and surface area increased, resulting in

higher extraction fraction. However, at high stirring rates, as the cells became smaller, the swelling increased, and the emulsion breakdown reduced the extraction rate. Figure 10b shows the effect of stirring speed on extraction, enrichment and emulsion swelling. With increasing the stirring speed, the water transfer from the external phase to the internal phase increases (e.g., swelling increases). On the other hand, the enrichment decreases with increasing mixer speed. At low speeds, the size of the emulsion cells increases and the mass transfer rate decreases [77].

Effect of W/O/W emulsion stirring time

Increasing the contact time, on the one hand, increases the mass transfer time and thus, the extraction rate is increased. On the other hand, increasing contact time due to internal phase leakage into the external phase causes swelling and consequently, emulsion breakdown and decreases extraction rate [78]. The important thing about the contact time in the emulsion liquid membrane process is that most of the extraction is done at the early stages of the process. The reason is the high mass transfer driving force at the beginning of the process. Figure 11a shows that the extraction rate increases with increasing time up to 15 min, and then, the extraction rate decreases. Almost most of the Hf extraction is performed in the first few minutes, and over time, the cells swell and the extraction decreases. As can be seen in Fig. 11a, as time increases, the swelling increases with the contact time, which can lead to emulsion breakdown. It is also important to note that contact time does not have a significant effect on enrichment.

Particle size test

Dynamic light scattering (DLS) apparatus was used to determine the emulsion particle size distribution in the experiments. A random sample of produced emulsions was analyzed with DLS, and the results are shown in Fig. 11b. According to Fig. 11b, the average particle size leaving the homogenizer at 16,000 rpm was 61 nm in size, indicating the formation of nano-emulsions in the experiments.

Modeling and optimization of hafnium ion extraction using design of experiment

In the classic one factor at a time (OFAT) method, to calculate various factors and find the optimal points of each factor, the response is examined for each factor, while all other factors are kept constant. Thus, the major weakness of this method is the lack of interaction between the factors and the existence of a large number of experiments [79]. This is a trial-and-error method and is not by any specific

Table 2 Levels of factors in the *D*-optimal design

Factors	Symbol	Unit	−1	0	+1
Carrier concentration	X_1	(v/v)	1.5	3	4.5
Surfactant concentration	X_2	(w/v)	2	3	4
W/O/W emulsion stirring time	X_3	min	10	15	20
W/O/W emulsion stirring speed	X_4	rpm	300	350	400
Emulsion volume/feed phase ratio	X_5	N/A	2	3	4

Table 3 *D*-optimal design matrix for Hf ion extraction

Run	A:X_1	B:X_2	C:X_3	D:X_4	E:X_5	Hf%
1	3	3	15	350	1	82.84
2	4.5	2	10	400	4	95.01
3	1.5	2	10	300	4	51.7
4	3	3	25	350	3	75.45
5	3	3	15	350	3	76.9
6	4.5	4	20	400	4	60.12
7	4.5	4	10	300	4	90.78
8	3	1	15	350	3	76.1
9	1.5	4	20	400	2	87.8
10	1.5	4	10	400	4	79.6
11	3	3	15	350	3	73.9
12	4.5	2	10	300	2	77.9
13	4.5	2	20	400	2	98.9
14	1.5	2	20	400	4	82.12
15	3	3	15	350	3	78.12
16	1.5	4	10	300	2	66.34
17	0	3	15	350	3	69.12
18	3	3	15	450	3	88.29
19	3	3	5	350	3	79.12
20	3	3	15	350	3	75.9
21	4.5	2	20	300	4	66.91
22	1.5	4	20	300	4	68.8
23	6	3	15	350	3	97.6
24	3	3	15	350	3	77.8
25	3	3	15	350	3	78.23
26	3	3	15	250	3	60.6
27	3	3	15	350	5	71.21
28	4.5	4	20	300	2	97.34
29	1.5	2	10	400	2	81.43
30	3	5	15	350	3	91.38
31	1.5	2	20	300	2	37.23
32	4.5	4	10	400	2	97.09

standard. As a result, the design of experiment method was used to overcome these problems. In the Design of Experiment (DOE) method, the factors are tested simultaneously in order to obtain an appropriate response [80]. For this purpose, response surface methodology (RSM) was used to find levels of influencing factors for testing. RSM is a set of statistical and mathematical methods useful for developing, improving and optimizing products and processes [81]. There are several methods to design experiments in RSM, such as Box–Behnken design (BBD) [82], central composite design (CCD) [83] and *D*-optimal design [84]. Of the methods mentioned, the *D*-optimal design method is particularly important because of the reduction in the number of samples and the optimization of the regression models. This method allows us to propose the best possible design using a criterion. The model used in the *D*-optimal method is generally the quadratic relation. The quadratic relation (Eq. 6) describes the behavior of the system:

$$Y = \beta_0 + \sum_{i=1}^{k} \beta_i X_i + \sum_{i=1}^{k} \sum_{j=1}^{k} \beta_{ij} X_i X_j + \sum_{i=1}^{k} \beta_{ii} x_i^2 + \varepsilon \quad (6)$$

where Y is the predicted response, β_0 is the constant coefficient, β_i is the linear effect, β_{ii} is the square effect, β_{ij} is the interaction effect, and ε is system error value. Equation 6 is solved using Design Expert 10 software to estimate the response of independent variables. The significance of each sentence in the regression equation is examined, and the analysis of variance (ANOVA) determines the significance of the model for each response [85]. Table 2 shows the factors influencing the test process at high and low levels. The five important factors studied are extraction concentration,
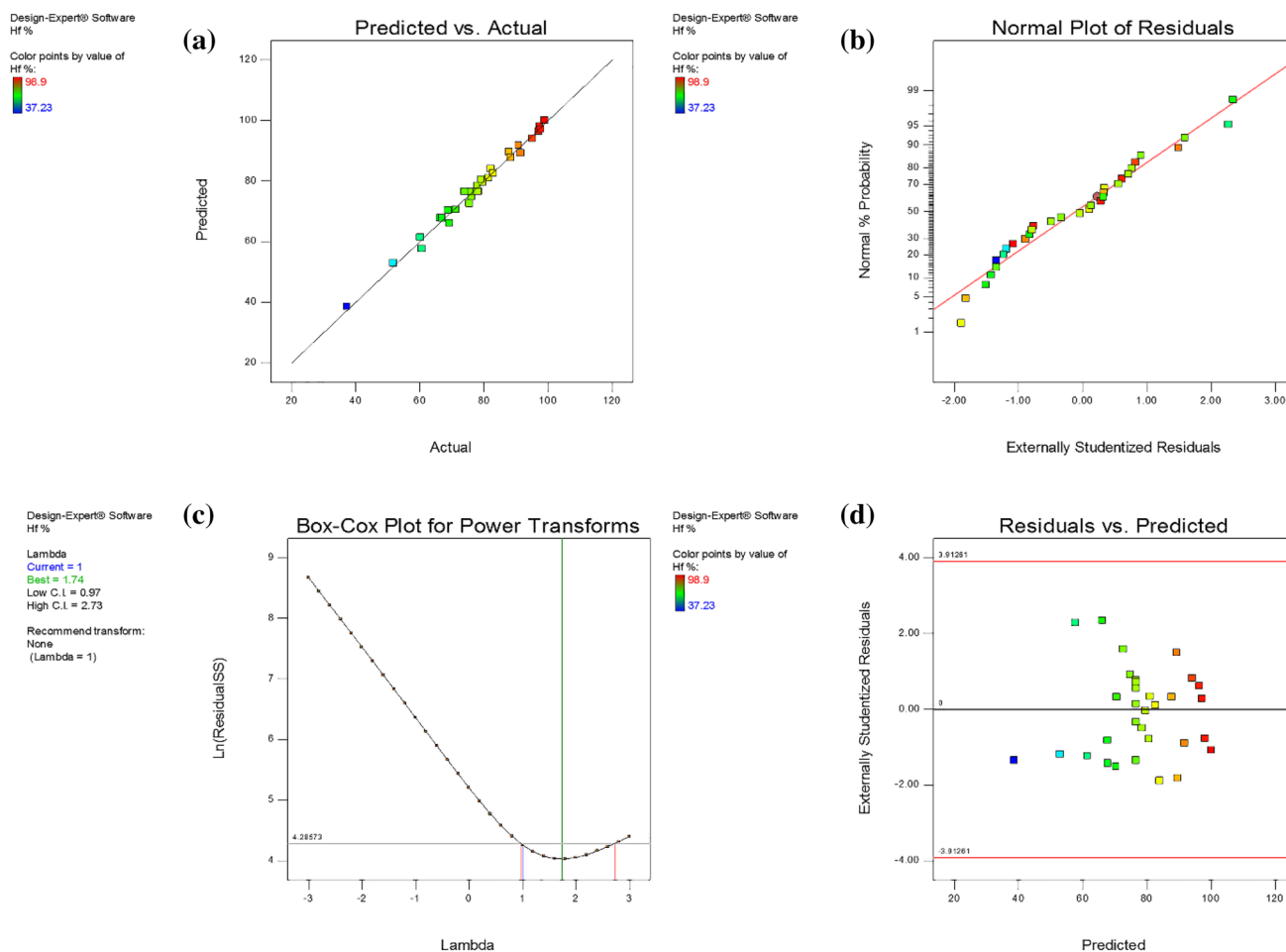
Fig. 12 Diagrams of **a** predict versus actual, **b** normal plot, **c** Box-Cox charts, **d** residual plot, for model adequacy in *D*-optimal method

surfactant concentration, the influence of mixing rate and time, and the effect of changes in the emulsion volume ratio on the external phase. Hafnium ion removal percentage was selected as the response. By placing five factors at two levels, 32 experiments were conducted, 20 of which were for non-central points and 12 central points for experiments involving hafnium ion extraction. The design matrix associated with the removal of hafnium ions in each test is shown in Table 3. ANOVA table and residual graphs in Fig. 12a–d were used to evaluate the model's accuracy and adequacy, respectively.

Model verification and adequacy

Model verification

Analysis of variance (ANOVA) was used to verify the model. The results of model variance analysis are shown in Tables 4 and 5. As can be seen in Table 4, the "model" *p* value (first row) is smaller than 0.05 (significant), while

the "lack of fit" is not significant. These together indicate the selected model is valid. According to Table 4, BC, CD, C^2 and E^2 factors have *p* value greater than 0.05, indicating that these statements are insignificant on the selected model. Due to the great advantage of the *D*-optimal design to enhance the selective model improvement, these insignificant sentences can be removed from the selected model. The reduced quadratic modality was applied to eliminate non-significant factors, using the backward algorithm in Design expert 10 software. Table 5 shows the analysis of variance of the reduced model. As can be seen, with the removal of the terms BC, CD, C^2 and E^2, the *F* value increased significantly, which indicated that the quality of the selected model was improved. In addition, the adjusted R-squared coefficient value for this model was 0.9752, indicating that the input factors expressed 97% of the response factor variability. This value has improved compared to the previous state. As well as, the graph of the predicted values versus the real values for the quadratic model is shown in Fig. 12a, which shows good correlation and proximity to the real values

Table 4 Analysis of variance (ANOVA) *D*-optimal for Hf ion removal

Source	Sum of squares	df	Mean square	F value	p value	
Model	5864.88	20	293.24	52.80	< 0.0001	Significant
A-X_1	1441.35	1	1441.35	259.53	< 0.0001	
B-X_2	317.04	1	317.04	57.09	< 0.0001	
C-X_3	95.88	1	95.88	17.26	0.0016	
D-X_4	1356.76	1	1356.76	244.30	< 0.0001	
E-X_5	217.50	1	217.50	39.16	< 0.0001	
AB	117.99	1	117.99	21.25	0.0008	
AC	73.92	1	73.92	13.31	0.0038	
AD	491.62	1	491.62	88.52	< 0.0001	
AE	287.56	1	287.56	51.78	< 0.0001	
BC	0.080	1	0.080	0.014	0.9067	
BD	935.90	1	935.90	168.52	< 0.0001	
BE	153.45	1	153.45	27.63	0.0003	
CD	3.75	1	3.75	0.68	0.4285	
CE	88.60	1	88.60	15.95	0.0021	
DE	142.50	1	142.50	25.66	0.0004	
A^2	43.38	1	43.38	7.81	0.0174	
B^2	50.43	1	50.43	9.08	0.0118	
C^2	2.69	1	2.69	0.48	0.5012	
D^2	30.08	1	30.08	5.42	0.0401	
E^2	3.96	1	3.96	0.71	0.4162	
Residual	61.09	11	5.55			
Lack of fit	47.07	6	7.85	2.80	0.1393	Not significant
Pure error	14.02	5	2.80			
Cor total	5925.97	31				

Std. dev. = 2.36; mean = 77.86; C.V. % = 3.03; PRESS = 1189.11; R-squared = 0.9897; adj R-squared = 0.9709; pred R-squared = 0.7993; adeq precision = 31.66

(pred R-squared 0.9121). As reported in Table 5, the mean of the data and its standard deviation are 77.86 and 2.28, respectively. The press value in this table is 520, indicating that the model conforms, to observations not included in the model estimates themselves. The value of the coefficient of variation is 2.80. A small value of the coefficient is desirable as it would imply that the data dispersion is not large. The signal value to the noise is introduced with adequate precision. In this proposed model, the adeq precision is 38.78. Finally, the quadratic equation of linear regression can be obtained with respect to Eq. 7. Given the values of Table 5, the coefficients of the linear regression equation will be as follows:

$$
\begin{aligned}
\text{Hf}\% = &+76.61 + 7.75 \times A + 3.63 \times B - 2.00 \times C \\
&+ 7.52 \times D - 3.01 \times E - 2.72 \times AB \\
&- 2.15 \times AC - 5.54 \times AD - 4.24 \times AE \\
&- 7.65 \times BD - 3.10 \times BE - 2.35 \\
&\times CE - 2.98 \times DE + 1.27 \times E^2 \\
&+ 1.36 \times B^2 - 0.96 \times D^2
\end{aligned}
\tag{7}
$$

Model adequacy

The next step is to check the adequacy and validity of the model. In this step, by analyzing the residuals and the other statistical analyzes, the suitability of the model is evaluated, and the applicability of the model is decided. The result of the model's adequacy checking makes it possible to say whether the model is appropriate, or that the original fitting needs to be modified. Therefore, regression analysis is a procedure with iteration and revision in which the data are guided to a model. Then, the quality of the fit is examined. The result will yield in the refinement in the fitting model or acceptance of the model. The best process regression model is a function that in addition to having high accuracy in communicating between input and output factors, is of lower order and simpler structure [86]. After we obtain the regression model of the problem, we must examine the model assumptions. If the model has statistical adequacy, the obtained equation is good. Otherwise, we should look for methods such as conversion to solve the model problems. Assumptions of regression models include: (1) residuals follow the normal distribution, (2) the residuals are independent

Table 5 Analysis of variance (ANOVA) optimized *D*-optimal for Hf ion removal

Source	Sum of squares	df	Mean square	F value	p value	
Model	5854.90	16	365.93	77.23	<0.0001	Significant
A-X_1	1441.35	1	1441.35	304.19	<0.0001	
B-X_2	317.04	1	317.04	66.91	<0.0001	
C-X_3	95.88	1	95.88	20.24	0.0004	
D-X_4	1356.76	1	1356.76	286.34	<0.0001	
E-X_5	217.50	1	217.50	45.90	<0.0001	
AB	117.99	1	117.99	24.90	0.0002	
AC	73.92	1	73.92	15.60	0.0013	
AD	491.62	1	491.62	103.76	<0.0001	
AE	287.56	1	287.56	60.69	<0.0001	
BD	935.90	1	935.90	197.52	<0.0001	
BE	153.45	1	153.45	32.39	<0.0001	
CE	88.60	1	88.60	18.70	0.0006	
DE	142.50	1	142.50	30.08	<0.0001	
A^2	47.75	1	47.75	10.08	0.0063	
B^2	55.18	1	55.18	11.65	0.0039	
D^2	27.45	1	27.45	5.79	0.0294	
Residual	71.07	15	4.74			
Lack of fit	57.06	10	5.71	2.04	0.2240	Not significant
Pure error	14.02	5	2.80			
Cor total	5925.97	31				

Std. dev. = 2.18; mean = 77.86; C.V. % = 2.80; PRESS = 520; R-squared = 0.9880; adj R-squared = 0.9752; pred R-squared = 0.9121; adeq precision = 38.78

of each other, and (3) the variance of the residuals is equal. The normal probability diagram (Fig. 12b) shows how the residuals follow a normal distribution. Even with natural data, some small deviations are expected. Curved, distinct patterns that can be identified with just one glance indicate that a better analysis can be obtained by performing a transformation on the response-dependent model. The Box-Cox curve is used to select the most appropriate power conversion function for the response factor. The lowest point in the Box-Cox chart represents the best value. When the ratio of maximum to minimum response is greater than 3, there will be a better ability to improve the model using the power conversion function. The remainder of the sum of squares of Fig. 12c is the best Box-Cox curve for λ (the lowest point in the graph). Nevertheless, because one is within confidence λ, no conversion is required. Figure 12d shows the graph of the residuals versus response prediction values and examines the assumption of constant variance. The funnel pattern can indicate that the variance between the residuals is not constant. In addition, the existence of a pattern at times may indicate that the model used is inappropriate. As shown in Fig. 12d, the scattering is random. Thus, the constant variance condition is established.

Investigate the relationship of response with relevant variables

Contour plot graphs

Contour plots influencing the test process can be seen in Figs. 13 and 14a–d, according to the ANOVA table. Contour plot two-dimensional diagrams such that it involves examining two factors simultaneously on the response rate, while the other factors are on their specified points (upper, lower and middle levels). In this chart is the interpretation in terms of colors. According to contour plots, to get the maximum response, two factors must be in the dark red range. Conclusions about the appropriate ranges of variables for the removal of hafnium ions according to the results of Figs. 13 and 14a–d are listed in Table 6. For example, in Fig. 13a we see two factors extraction concentration (X_1) and surfactant concentration (X_2) with response rate, while factors X_4, X_3 and X_5 are in the lower, middle and lower positions, respectively. By looking at this graph, we find that if factor X_1 is at its highest level (3.5–5) and factor (X_2) is at its highest level (3–5), the highest response rate for hafnium ion recovery would be achieved.
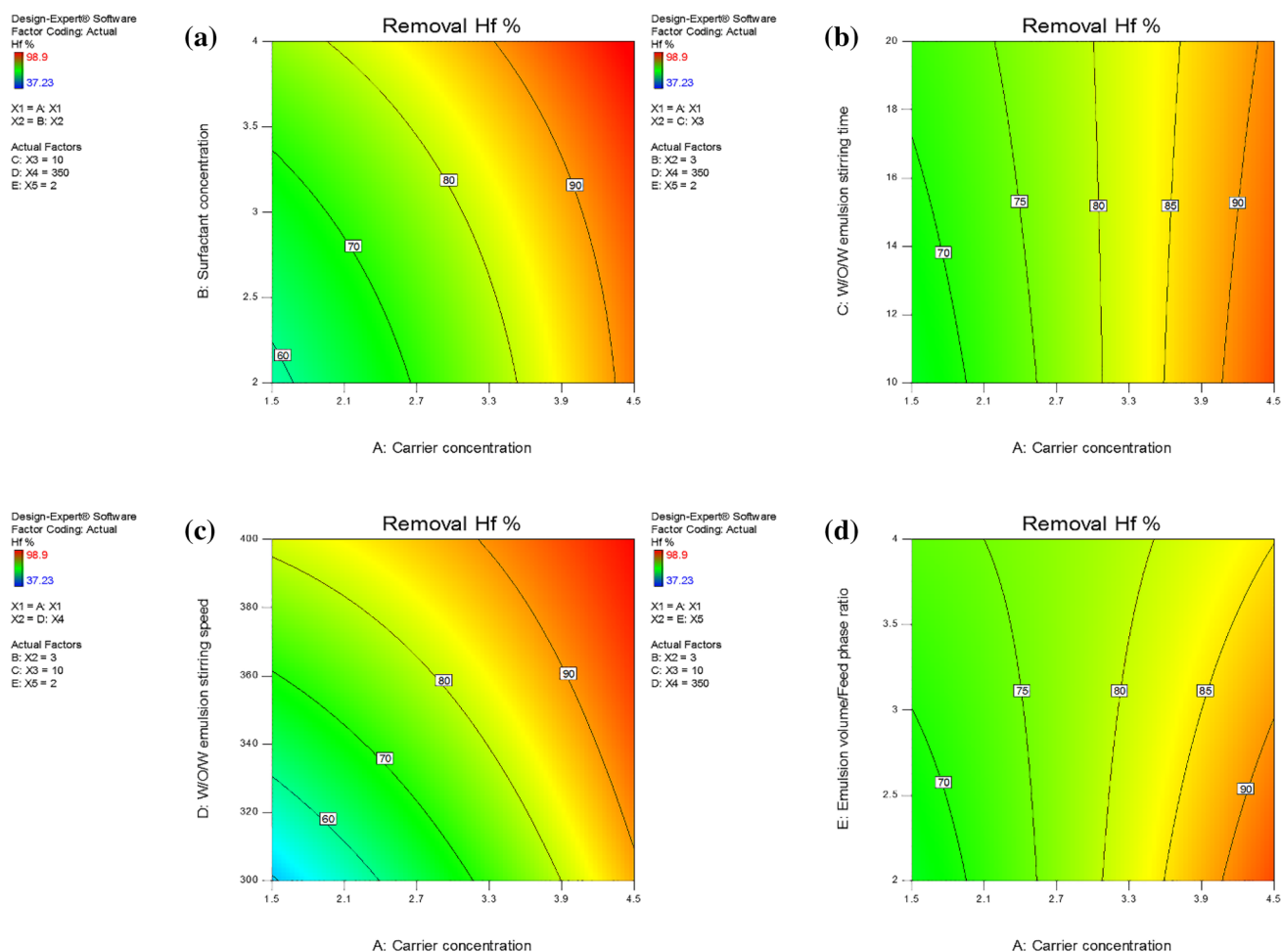
Fig. 13 Diagrams of the counter plot **a** carrier concentration (X_1) versus surfactant concentration (X_2), **b** carrier concentration (X_1) versus W/O/W emulsion stirring time (X_3), **c** carrier concentration (X_1) ver-

sus W/O/W emulsion stirring speed (X_4), **d** carrier concentration (X_1) versus emulsion phase/feed phase volume ratio (X_5) with response rate

Optimization

According to the design of the experimental results, the optimum points for maximum extraction are presented in Fig. 15, which results in the highest response. As shown in Fig. 15, the carrier concentration (4.49), surfactant concentration (3.90), W/O/W emulsion stirring time (11.49), W/O/W emulsion stirring speed (310.54) and emulsion volume/feed phase ratio (2) will have the highest extraction rate of 99.84%. One experiment was carried out with the conditions suggested by Design Expert 10 to achieve the highest extraction rate. The extraction rate of the test was measured to be ~98.2% which is very close to the predicted value of 99.84%.

Conclusion

The emulsion liquid membrane method is an effective method for the separation of low-concentration metals, in which the separation method is quick, and the extraction rate is high. It is noteworthy that it is important to select the appropriate carrier material that can be complexed with the heavy metal molecules to separate them. In this study, Hafnium metal was captured from water and released into a solution of water and HCl using ELM method. Since the extraction of hafnium metal has not been carried out using the emulsion liquid membrane method so far, the effect of each of the process factors include polymer concentration, surfactant concentration, emulsification time, internal phase
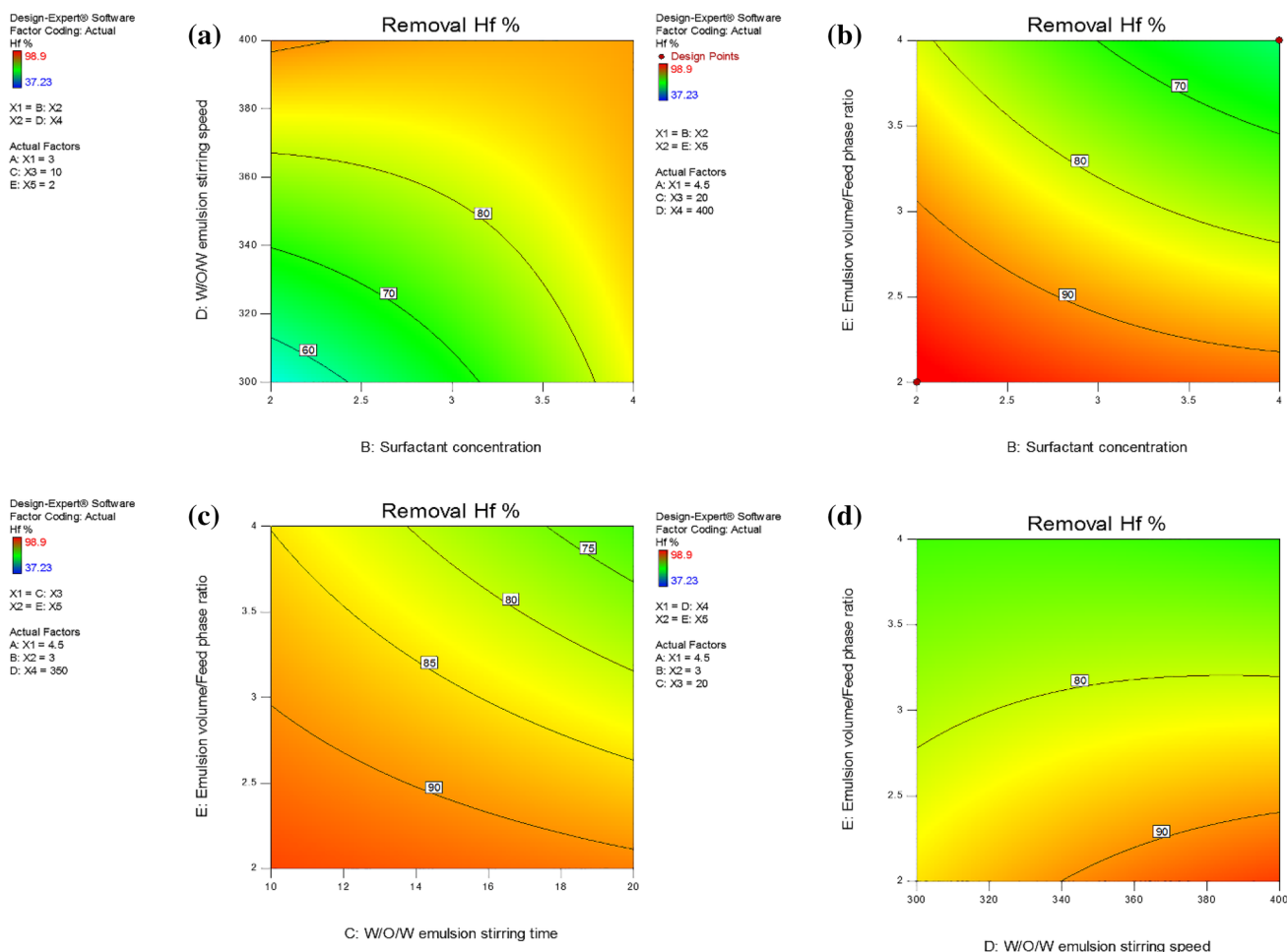
Fig. 14 Diagrams of the counter plot **a** surfactant concentration (X_2) versus W/O/W emulsion stirring speed (X_4), **b** surfactant concentration (X_2) versus emulsion phase/feed phase volume ratio (X_5), **c** W/O/W emulsion stirring time (X_3) versus emulsion phase/feed phase volume ratio (X_5), **d** W/O/W emulsion stirring speed (X_4) versus emulsion phase/feed phase volume ratio (X_5) with response rate

Table 6 Suitable ranges of variables for the response

Factors	Symbol	Unit	Factors ranges for high Hf removal	Supporting graphs
Carrier concentration	X_1	(v/v)	3.5–4.5	Figure 14a–d
Surfactant concentration	X_2	(w/v)	3–5	Figures 14a–15a, b
W/O/W emulsion stirring time	X_3	min	10–15	Figures 14b–15c, d
W/O/W emulsion stirring speed	X_4	rpm	300–400	Figures 14c–15a
Emulsion volume/feed phase ratio	X_5	N/A	2–3	Figures 14d–15c, d

concentration (stripping phase) and volumetric phase ratio. The oil into the internal phase on the membrane stability was evaluated. The optimum conditions for emulsion stability were polymer concentration 3 wt%, surfactant concentration 4% (w/v), contact time 15 min, internal phase HCl 0.8 M concentration and the volume ratio of the membrane to feed (1:1). As well as, the effect of carrier concentration, surfactant concentration, W/O/W emulsion stirring time and

speed, and emulsion volume/feed phase ratio on extraction and enrichment were investigated. In addition, optimum separation conditions in ELM process were obtained as: carrier concentration 4.5% (v/v), surfactant concentration 4% (w/v), W/O/W emulsion stirring time (15 min), W/O/W emulsion stirring speed (350 rpm) and emulsion phase/feed phase volume ratio (20/100). *D*-optimal test design via Design Experiment 10 software was used to optimize the factors
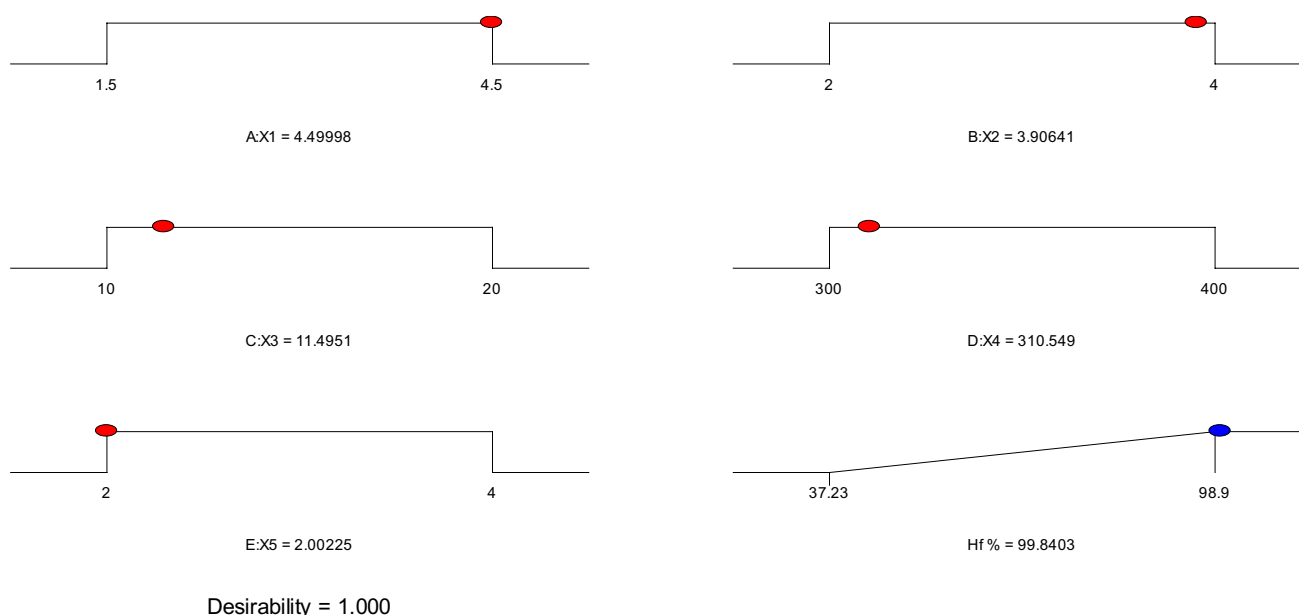
A:X1 = 4.49998

B:X2 = 3.90641

C:X3 = 11.4951

D:X4 = 310.549

E:X5 = 2.00225

Hf % = 99.8403

Desirability = 1.000

Fig. 15 The optimum points of the factors to maximize the response

affecting the tests of ELM. Influence of parameters such as carrier concentration, surfactant concentration, contact time, stirring rate and the membrane-to-volume ratio was studied using the results obtained from experiments and evaluation with optimum points software to reach the maximum. The suggested values by the software to get 0.99 extraction fraction were as follows: carrier concentration ~ 4.5% (v/v), surfactant concentration 3.90% (w/v), W/O/W emulsion stirring time (~ 12 min), W/O/W emulsion stirring speed ~ 310 rpm and emulsion phase-to-feed phase volume ratio (20/100). The experiments with the suggested conditions yielded ~ 0.98 extraction.

Compliance with ethical standards

References

1. C. Fonseca Couto, L.C. Lange, M.C. Santos Amaral, A critical review on membrane separation processes applied to remove pharmaceutically active compounds from water and wastewater. J. Water Process Eng. **26**, 156–175 (2018). https://doi.org/10.1016/j.jwpe.2018.10.010
2. T.C. Zhang, R.Y. Surampalli, S. Vigneswaran, R. Tyagi, S. Leong Ong, C. Kao, *Membrane Technology and Environmental Applications* (American Society of Civil Engineers, New York, 2012)
3. D. Nasirian, I. Salahshoori, M. Sadeghi, N. Rashidi, M. Hassanzadeganroudsari, Investigation of the gas permeability properties from polysulfone/polyethylene glycol composite membrane. Polym. Bull. (2019). https://doi.org/10.1007/s00289-019-03031-3
4. I. Salahshoori, D. Nasirian, N. Rashidi, M.K. Hossain, A. Hatami, M. Hassanzadeganroudsari, The effect of silica nanoparticles on polysulfone–polyethylene glycol (PSF/PEG) composite membrane on gas separation and rheological properties of nanocomposites. Polym. Bull. (2020). https://doi.org/10.1007/s00289-020-03255-8
5. A. Hatami, I. Salahshoori, N. Rashidi, D. Nasirian, The effect of ZIF-90 particle in Pebax/PSF composite membrane on the transport properties of CO_2, CH_4 and N_2 gases by molecular dynamics simulation method. Chin. J. Chem. Eng. (2019). https://doi.org/10.1016/j.cjche.2019.12.011
6. S. Mondal, M.K. Purkait, S. De, Emulsion liquid membrane, in *Advances in Dye Removal Technologies*, ed. by S. Mondal, M.K. Purkait, S. De (Springer, Singapore, 2018), pp. 313–323. https://doi.org/10.1007/978-981-10-6293-3_10
7. A.L. Ahmad, A. Kusumastuti, C.J.C. Derek, B.S. Ooi, Emulsion liquid membrane for heavy metal removal: an overview on emulsion stabilization and destabilization. Chem. Eng. J. **171**(3), 870–882 (2011). https://doi.org/10.1016/j.cej.2011.05.102
8. M.B. Rosly, N. Jusoh, N. Othman, H.A. Rahman, N.F.M. Noah, R.N.R. Sulaiman, Effect and optimization parameters of phenol removal in emulsion liquid membrane process via fractional-factorial design. Chem. Eng. Res. Des. **145**, 268–278 (2019). https://doi.org/10.1016/j.cherd.2019.03.007
9. P. Dzygiel, P. Wieczorek, Extraction of amino acids with emulsion liquid membranes using industrial surfactants and lecithin as stabilisers. J. Membr. Sci. **172**(1), 223–232 (2000). https://doi.org/10.1016/S0376-7388(00)00330-6
10. N. Othman, H. Mat, M. Goto, Separation of silver from photographic wastes by emulsion liquid membrane system. J. Membr. Sci. **282**(1), 171–177 (2006). https://doi.org/10.1016/j.memsci.2006.05.020
11. A. Kargari, T. Kaghazchi, B. Mardangahi, M. Soleimani, Experimental and modeling of selective separation of gold(III) ions

from aqueous solutions by emulsion liquid membrane system. J. Membr. Sci. **279**(1), 389–393 (2006). https://doi.org/10.1016/j.memsci.2005.12.027

12. H. Valdés, J. Romero, J. Sanchez, S. Bocquet, G.M. Rios, F. Valenzuela, Characterization of chemical kinetics in membrane-based liquid–liquid extraction of molybdenum(VI) from aqueous solutions. Chem. Eng. J. **151**(1), 333–341 (2009). https://doi.org/10.1016/j.cej.2009.04.012

13. A. Srivastava, A. Bhagat, U. Sharma, R.K. Dohare, K. Singh, S. Upadhyaya, Comparative study of arsenic(V) removal from aqueous solution using Aliquat-336 and 2-ethyl hexanol through emulsion liquid membrane. J. Water Process Eng. **16**, 64–68 (2017). https://doi.org/10.1016/j.jwpe.2016.12.007

14. K. Wongkaew, V. Mohdee, U. Pancharoen, A. Arpornwichanop, A.W. Lothongkum, Separation of platinum(IV) across hollow fiber supported liquid membrane using non-toxic diluents: mass transfer and thermodynamics. J. Ind. Eng. Chem. **54**, 278–289 (2017). https://doi.org/10.1016/j.jiec.2017.06.002

15. F. Moyo, R. Tandlich, Daphnia pulex toxicity testing of ethylenediaminetetraacetic acid tetrasodium salt dihydrate and the wastewater effluent from extraction of rhodium using emulsion liquid membranes. Int. J. Environ. Res. **8**(4), 1019–1026 (2014)

16. A.L. Ahmad, M.M.H. Shah Buddin, B.S. Ooi, A. Kusumastuti, Utilization of environmentally benign emulsion liquid membrane (ELM) for cadmium extraction from aqueous solution. J. Water Process Eng. **15**, 26–30 (2017). https://doi.org/10.1016/j.jwpe.2016.05.010

17. A. Hachemaoui, K. Belhamel, Simultaneous extraction and separation of cobalt and nickel from chloride solution through emulsion liquid membrane using Cyanex 301 as extractant. Int. J. Miner. Process. **161**, 7–12 (2017). https://doi.org/10.1016/j.minpro.2017.02.002

18. H. Ma, O. Kökkılıç, K.E. Waters, The use of the emulsion liquid membrane technique to remove copper ions from aqueous systems using statistical experimental design. Miner. Eng. **107**, 88–99 (2017). https://doi.org/10.1016/j.mineng.2016.10.014

19. M.D. Asl, I. Salahshoori, A. Seyfaee, A. Hatami, A.A. Golbarari, Experimental results and optimization via design of experiment (DOE) of the copper ion recovery from aqueous solutions using emulsion liquid membrane (ELM) method. Desalination and Water Treatment (in press) (2020)

20. S.S. Kulkarni, V.A. Juvekar, S. Mukhopadhyay, Intensification of emulsion liquid membrane extraction of uranium(VI) by replacing nitric acid with sodium nitrate solution. Chem. Eng. Process. Process Intens. **125**, 18–26 (2018). https://doi.org/10.1016/j.cep.2017.12.021

21. N.F.M. Noah, N. Othman, N. Jusoh, Highly selective transport of palladium from electroplating wastewater using emulsion liquid membrane process. J. Taiwan Inst. Chem. Eng. **64**, 134–141 (2016). https://doi.org/10.1016/j.jtice.2016.03.047

22. A. Choudhury, S. Sengupta, C. Bhattacharjee, S. Datta, Extraction of hexavalent chromium from aqueous stream by emulsion liquid membrane (ELM). Sep. Sci. Technol. **45**(2), 178–185 (2010). https://doi.org/10.1080/01496390903409617

23. F. Valenzuela, J. Cabrera, C. Basualto, J. Sapag, J. Romero, J. Sánchez, G. Rios, Separation of zinc ions from an acidic mine drainage using a stirred transfer cell-type emulsion liquid membrane contactor. Sep. Sci. Technol. **42**(2), 363–377 (2007). https://doi.org/10.1080/01496390601069887

24. A. Yadollahi, M. Torab-Mostaedi, K. Saberyan, A. Charkhi, F. Zahakifar, Intensification of zirconium and hafnium separation through the hollow fiber renewal liquid membrane technique using synergistic mixture of TBP and Cyanex-272 as extractant. Chin. J. Chem. Eng. **27**(8), 1817–1827 (2019). https://doi.org/10.1016/j.cjche.2018.12.018

25. P. Davoodi-Nasab, A. Rahbar-Kelishami, J. Safdari, H. Abolghasemi, Selective separation and enrichment of neodymium and gadolinium by emulsion liquid membrane using a novel extractant CYANEX® 572. Miner. Eng. **117**, 63–73 (2018). https://doi.org/10.1016/j.mineng.2017.11.008

26. M. Chakraborty, C. Bhattacharya, S. Datta, Emulsion liquid membranes: definitions and classification, theories, module design, applications, new directions and perspectives, in *Liquid Membranes*, vol. 4, ed. by V.S. Kislik (Elsevier, Amsterdam, 2010), pp. 141–199. https://doi.org/10.1016/B978-0-444-53218-3.00004-0

27. O.I. Lee, The mineralogy of hafnium. Chem. Rev. **5**(1), 17–37 (1928)

28. C.E. Curtis, *Bibliography of hafnium oxide, hafnium silicate and hafnium carbide* (Oak Ridge National Lab, Oak Ridge, 1952)

29. J. van Liempt, Hafnium oxide in tungsten filaments. Nature **115**(2884), 194 (1925)

30. C.M. Swamidoss, D.D. Malkhede, A highly selective liquid–liquid extraction technique for the extraction and separation of hafnium(IV) with hexaacetato calix(6)arene. Orient. J. Chem. **26**, 117–122 (2010)

31. K. Mimura, K. Matsumoto, M. Isshiki, Purification of hafnium by hydrogen plasma arc melting. Mater. Trans. **52**(2), 159–165 (2011)

32. S. Shishkin, T. Shishkina, G. Buklanov, S. Dmitriev, G.Y. Starodub, Separation of carrier free 178 W from α-particle activated hafnium with TBP impregnated resin. Czech J. Phys. **53**(1), A425–A427 (2003)

33. Z.-G. Xu, Y.-K. Wu, J.-D. Zhang, L. Zhang, L.-J. Wang, Equilibrium and kinetic data of adsorption and separation for zirconium and hafnium onto MIBK extraction resin. Trans. Nonferrous Met. Soc. China **20**(8), 1527–1533 (2010)

34. L. Beer, D. van der Westhuizen, H. Krieg, Solvent extraction and separation of hafnium from zirconium using Ionquest 801. J. South Afr. Inst. Min. Metall. **116**, 93–99 (2016). https://doi.org/10.17159/2411-9717/2016/v116n1a14

35. B. Nandi, N.R. Das, S.N. Bhattacharyya, Solvent extraction of zirconium and hafnium. Solv. Extr. Ion Exchange **1**(1), 141–202 (1983). https://doi.org/10.1080/07366298308918397

36. M. Khan, A.A. Ali, Liquid–liquid extraction of Hf(IV) from nitric acid with dibutylsulfoxide in cyclohexane. Radiochim. Acta (2002). https://doi.org/10.1524/ract.2002.90.5_2002.297

37. A.A. Nayl, Y. El-Nadi, J. Daoud, Extraction and separation of Zr(IV) and Hf(IV) from nitrate medium by some CYANEX extractants. Sep. Sci. Technol. **44**, 2956–2970 (2009). https://doi.org/10.1080/01496390903014169

38. J. Amaral, C. Morais, Study of zirconium and hafnium separation by solvent extraction technique from nitric and hydrochloric solutions with acid, basic and neutral extractants. World J. Eng. Technol. **04**, 138–150 (2016). https://doi.org/10.4236/wjet.2016.43D017

39. J. Zhao, T. Yang, H. Zhang, G. Sun, Y. Cui, Preferential extraction of hafnium over zirconium with D2EHPA through selective complexation of organic acids. J. Radioanal. Nucl. Chem. **321**(1), 333–339 (2019). https://doi.org/10.1007/s10967-019-06585-8

40. R. Banda, H.Y. Lee, M.S. Lee, Separation of Zr from Hf in hydrochloric acid solution using amine-based extractants. Ind. Eng. Chem. Res. **51**(28), 9652–9660 (2012). https://doi.org/10.1021/ie3008264

41. C. Tunsu, Hydrometallurgical recovery of rare earth elements from fluorescent lamp waste fractions. Department of chemistry and chemical engineering, Chalmers University of Technology Gutenburg, Sweden (2016)

42. Y. Wang, F. Li, Z. Zhao, Y. Dong, X. Sun, The novel extraction process based on CYANEX® 572 for separating heavy rare

earths from ion-adsorbed deposit. Sep. Purif. Technol. **151**, 303–308 (2015). https://doi.org/10.1016/j.seppur.2015.07.063

43. P.S. Kulkarni, V.V. Mahajani, Application of liquid emulsion membrane (LEM) process for enrichment of molybdenum from aqueous solutions. J. Membr. Sci. **201**(1), 123–135 (2002). https://doi.org/10.1016/S0376-7388(01)00720-7

44. K. Abbassian, A. Kargari, Effect of polymer addition to membrane phase to improve the stability of emulsion liquid membrane for phenol pertraction. Desalin. Water Treat. **57**(7), 2942–2951 (2016). https://doi.org/10.1080/19443994.2014.983981

45. Y.S. Ng, N.S. Jayakumar, M.A. Hashim, Performance evaluation of organic emulsion liquid membrane on phenol removal. J. Hazard. Mater. **184**(1), 255–260 (2010). https://doi.org/10.1016/j.jhazmat.2010.08.030

46. A. Barkat, B. Khan, A. Naveed, H. Muhammad, H.M.S. Khan, K. Waseem, T. Mahmood, A. Rasul, M. Iqbal, H. Khan, Basics of pharmaceutical emulsions: a review. Afr. J. Pharm. Pharmacol. **525**, 2715–2725 (2011). https://doi.org/10.5897/AJPP11.698

47. A.L. Ahmad, A. Kusumastuti, C.J.C. Derek, O. Seng, Emulsion liquid membrane for heavy metal removal: an overview on emulsion stabilization and destabilization. Chem. Eng. J. Chem. Eng. J. **171**, 870–882 (2011). https://doi.org/10.1016/j.cej.2011.05.102

48. S. Gupta, P.B. Khandale, M. Chakraborty, Application of emulsion liquid membrane for the extraction of diclofenac and relationship with the stability of water-in-oil emulsions. J. Dispers. Sci. Technol. (2019). https://doi.org/10.1080/01932691.2019.1579655

49. Y. Park, Development and optimization of novel emulsion liquid membranes stabilized by non-Newtonian conversion in Taylor-Couette flow for extraction of selected organic and metallic contaminants, Georgia Institute of Technology (2006)

50. J. Barad, M. Chakraborty, H.-J. Bart, Stability and performance study of water-in-oil-in-water emulsion: extraction of aromatic amines. Ind. Eng. Chem. Res. **49**, 5808–5815 (2010). https://doi.org/10.1021/ie901698u

51. Y. Park, L.J. Forney, J.H. Kim, A.H.P. Skelland, Optimum emulsion liquid membranes stabilized by non-Newtonian conversion in Taylor–Couette flow. Chem. Eng. Sci. **59**(24), 5725–5734 (2004). https://doi.org/10.1016/j.ces.2004.06.015

52. A.H.P. Skelland, X. Meng, A new solution to emulsion liquid membrane problems by non-Newtonian conversion. AIChE J. **42**(2), 547–561 (1996). https://doi.org/10.1002/aic.690420224

53. B. Brugger, W. Richtering, Emulsions stabilized by stimuli-sensitive poly(*N*-isopropylacrylamide)-*co*-methacrylic acid polymers: microgels versus low molecular weight polymers. Langmuir ACS J. Surfaces Colloids **24**(15), 7769–7777 (2008). https://doi.org/10.1021/la800522h

54. S.C. Lee, S.M. Yeo, Role of dilute polymer solution in penicillin G extraction by emulsion liquid membranes. J. Ind. Eng. Chem. **8**(2), 114–119 (2002)

55. H.R. Mortaheb, M.H. Amini, F. Sadeghian, B. Mokhtarani, H. Daneshyar, Study on a new surfactant for removal of phenol from wastewater by emulsion liquid membrane. J. Hazard. Mater. **160**(2–3), 582–588 (2008)

56. H.R. Mortaheb, H. Kosuge, B. Mokhtarani, M.H. Amini, H.R. Banihashemi, Study on removal of cadmium from wastewater by emulsion liquid membrane. J. Hazard. Mater. **165**(1–3), 630–636 (2009)

57. A.H.P. Skelland, X. Meng, Non-Newtonian conversion solves problems of stability, permeability, and swelling in emulsion liquid membranes. J. Membr. Sci. **158**(1), 1–15 (1999). https://doi.org/10.1016/S0376-7388(98)00332-9

58. F. Nakashio, M. Goto, M. Matsumoto, J. Irie, K. Kondo, Role of surfactants in the behavior of emulsion liquid membranes—development of new surfactants. J. Membr. Sci. **38**(3), 249–260 (1988). https://doi.org/10.1016/S0376-7388(00)82423-0

59. F. Goodarzi, S. Zendehboudi, A comprehensive review on emulsions and emulsion stability in chemical and energy industries. Can. J. Chem. Eng. **97**(1), 281–309 (2019)

60. A. Dâas, O. Hamdaoui, Extraction of anionic dye from aqueous solutions by emulsion liquid membrane. J. Hazard. Mater. **178**(1–3), 973–981 (2010)

61. W. Yinhua, X. Zhang, Swelling determination of W/O/W emulsion liquid membranes. J. Membr. Sci. **196**, 185–201 (2002). https://doi.org/10.1016/S0376-7388(01)00554-3

62. A. Dâas, O. Hamdaoui, Extraction of bisphenol A from aqueous solutions by emulsion liquid membrane. J. Membr. Sci. **348**(1), 360–368 (2010). https://doi.org/10.1016/j.memsci.2009.11.026

63. A.L. Ahmad, M.M.H. Shah Buddin, B.S. Ooi, A. Kusumastuti, Cadmium removal from aqueous solution by emulsion liquid membrane (ELM): influence of emulsion formulation on cadmium removal and emulsion swelling. Desalin. Water Treat. **57**(58), 28274–28283 (2016). https://doi.org/10.1080/19443994.2016.1179674

64. N. Jusoh, N. Othman, Stability of water-in-oil emulsion in liquid membrane prospect. Malays. J. Fundam. Appl. Sci. (2017). https://doi.org/10.11113/mjfas.v12n3.429

65. A.L. Ahmad, A. Kusumastuti, C.J.C. Derek, B.S. Ooi, Emulsion liquid membrane for cadmium removal: studies on emulsion diameter and stability. Desalination **287**, 30–34 (2012). https://doi.org/10.1016/j.desal.2011.11.002

66. S. Laki, A. Bbbbbb, S. Madaeni, M. Niroomanesh, Separation of manganese from aqueous solution using emulsion liquid membrane. RSC Adv. (2015). https://doi.org/10.1039/C5RA08547K

67. Z.-Y. Ooi, N. Othman, C.-L. Choo, The role of internal droplet size on emulsion stability and the extraction performance of kraft lignin removal from pulping wastewater in emulsion liquid membrane process. J. Dispers. Sci. Technol. **37**(4), 544–554 (2016). https://doi.org/10.1080/01932691.2015.1050728

68. A. Dâas, O. Hamdaoui, Extraction of bisphenol A from aqueous solutions by emulsion liquid membrane. J. Membr. Sci. **348**(1–2), 360–368 (2010)

69. S.C. Lee, Effect of volume ratio of internal aqueous phase to organic membrane phase (w/o ratio) of water-in-oil emulsion on penicillin G extraction by emulsion liquid membrane. J. Membr. Sci. **163**(2), 193–201 (1999). https://doi.org/10.1016/S0376-7388(99)00182-9

70. M. Hasan, Y. Selim, K. Mohamed, Removal of chromium from aqueous waste solution using liquid emulsion membrane. J. Hazard. Mater. **168**(2–3), 1537–1541 (2009)

71. P.S. Kankekar, S.J. Wagh, V.V. Mahajani, Process intensification in extraction by liquid emulsion membrane (LEM) process: a case study; enrichment of ruthenium from lean aqueous solution. Chem. Eng. Process. **49**(4), 441–448 (2010). https://doi.org/10.1016/j.cep.2010.02.005

72. M.A. Malik, M.A. Hashim, F. Nabi, Extraction of metal ions by ELM separation technology. J. Dispers. Sci. Technol. **33**(3), 346–356 (2012). https://doi.org/10.1080/01932691.2011.567148

73. Y. Wang, F. Li, Z. Zhao, Y. Dong, X. Sun, The novel extraction process based on CYANEX® 572 for separating heavy rare earths from ion-adsorbed deposit. Sep. Purif. Technol. (2015). https://doi.org/10.1016/j.seppur.2015.07.063

74. I. Bhatti, K. Qureshi, K.S.N. Kamarudin, A.A. Bazmi, A.W. Bhutto, F. Ahmad, M. Lee, Innovative method to prepare a stable emulsion liquid membrane for high CO_2 absorption and its performance evaluation for a natural gas feed in a rotating disk contactor. J. Nat. Gas Sci. Eng. **34**, 716–732 (2016)

75. I. Torotwa, C. Ji, A study of the mixing performance of different impeller designs in stirred vessels using computational fluid dynamics. Designs **2**(1), 10 (2018)

76. B. Mokhtari, K. Pourabdollah, Inclusion separation of alkali metals in emulsion liquid membranes by nanobaskets of calix [4] crown-3. Braz. J. Chem. Eng. **29**(4), 783–793 (2012)

77. J. Yan, R. Pal, Isotonic swelling behavior of W/O/W emulsion liquid membranes under agitation conditions. J. Membr. Sci. **213**, 1–12 (2003). https://doi.org/10.1016/S0376-7388(02)00501-X

78. N. Noah, N.N. Othman, Emulsion stability of palladium extraction containing cyanex 302 as a mobile carrier in emulsion liquid membrane process. Chem. Eng. Trans. **56**, 1069–1074 (2017)

79. L.M. Collins, J.J. Dziak, R. Li, Design of experiments with multiple independent variables: a resource management perspective on complete and reduced factorial designs. Psychol. Methods **14**(3), 202 (2009)

80. J.R. Wagner, E.M. Mount, H.F. Giles, 25-Design of experiments, in *Extrusion*, 2nd edn., ed. by J.R. Wagner, E.M. Mount, H.F. Giles (William Andrew Publishing, Oxford, 2014), pp. 291–308. https://doi.org/10.1016/B978-1-4377-3481-2.00025-9

81. M.A. Bezerra, R.E. Santelli, E.P. Oliveira, L.S. Villar, L.A. Escaleira, Response surface methodology (RSM) as a tool for optimization in analytical chemistry. Talanta **76**(5), 965–977 (2008)

82. S.C. Ferreira, R. Bruns, H. Ferreira, G. Matos, J. David, G. Brandao, E.P. da Silva, L. Portugal, P. Dos Reis, A. Souza, Box-Behnken design: an alternative for the optimization of analytical methods. Anal. Chim. Acta **597**(2), 179–186 (2007)

83. H. Ahn, Central composite design for the experiments with replicate runs at factorial and axial points, in *Industrial Engineering, Management Science and Applications*, ed. by M. Gen, K.J. Kim, X. Huang, Y. Hiroshi (Springer, Berlin, 2015), pp. 969–979

84. P.F. de Aguiar, B. Bourguignon, M.S. Khots, D.L. Massart, R. Phan-Than-Luu, *D*-optimal designs. Chemometr. Intell. Lab. Syst. **30**(2), 199–210 (1995). https://doi.org/10.1016/0169-7439(94)00076-X

85. L. St, S. Wold, Analysis of variance (ANOVA). Chemometr. Intell. Lab. Syst. **6**(4), 259–272 (1989)

86. J. Martin, D.D.R. De Adana, A.G. Asuero, Fitting models to data: residual analysis, a primer. Chapter **7**, 133 (2017)